Cellular and molecular characterization of multiplex autism in human induced pluripotent stem cell-derived neurons

Emily M.A. Lewis[1]*, Kesavan Meganathan[1]*, Dustin Baldridge[2], Paul Gontarz[1], Bo Zhang[1], Azad Bonni[3], John N. Constantino[4] and Kristen L. Kroll[1**]

*Contributed equally

**Corresponding Author

Departments of [1]Developmental Biology, [2]Pediatrics, [3]Neuroscience, and [4]Psychiatry
Washington University School of Medicine, St. Louis, MO 63110

Emily M. A. Lewis – e.lewis@wustl.edu

Kesavan Meganathan - meganathank@wustl.edu

Dustin Baldridge - dbaldri@wustl.edu

Paul Gontarz - pgontarz@wustl.edu

Bo Zhang - bzhang29@wustl.edu

Azad Bonni - bonni@wustl.edu

John N. Constantino - constantino@wustl.edu

Corresponding Author:

Kristen L. Kroll - kkroll@wustl.edu

Phone – 314-362-7045

Fax – 314-362-7058

Abstract

Background: Autism spectrum disorder (ASD) is a neurodevelopmental disorder with pronounced heritability in the general population. This is largely attributable to effects of polygenic susceptibility, with inherited liability exhibiting distinct sex differences in phenotypic expression. Attempts to model ASD in human cellular systems have principally involved rare *de novo* mutations associated with ASD phenocopies. However, by definition, these models are not representative of polygenic liability, which accounts for the vast share of population-attributable risk.

Methods: Here, we performed what is, to our knowledge, the first attempt to model multiplex autism using patient-derived induced pluripotent stem cells (iPSCs) in a family manifesting incremental degrees of phenotypic expression of inherited liability (absent, intermediate, severe). The family members share an inherited variant of unknown significance in *GPD2*, a gene that was previously associated with developmental disability but here is insufficient by itself to cause ASD. iPSCs from three first-degree relatives and an unrelated control were differentiated into both cortical excitatory (cExN) and cortical inhibitory (cIN) neurons, and cellular phenotyping and transcriptomic analysis were conducted.

Results: cExN neurospheres from the two affected individuals were reduced in size, compared to those derived from unaffected related and unrelated individuals. This reduction was, at least in part, due to increased apoptosis of cells from affected individuals upon initiation of cExN neural induction. Likewise, cIN neural progenitor cells from affected individuals exhibited increased apoptosis, compared to both unaffected individuals. Transcriptomic analysis of both cExN and cIN neural progenitor cells revealed distinct molecular signatures associated with affectation, including misregulation of suites of genes associated with neural development, neuronal function, and behavior, as well as altered expression of ASD risk-associated genes.

Conclusions: We have provided evidence of morphological, physiological, and transcriptomic signatures of polygenic liability to ASD from an analysis of cellular models derived from a multiplex autism family. ASD is commonly inherited on the basis of additive genetic liability. Therefore, identifying convergent cellular and molecular phenotypes resulting from polygenic and monogenic susceptibility may provide a critical bridge for determining which of the disparate effects of rare highly deleterious mutations might also apply to common autistic syndromes.

Keywords: Multiplex autism, iPSC modeling, neurodevelopment, cortical excitatory neurons, cortical inhibitory neurons, transcriptomics, gene networks.

Background

Autism spectrum disorder (ASD) is a neurodevelopmental disorder with a complex and poorly understood etiology (1-3). Behavioral and imaging studies have been valuable for defining deficits in affected individuals and characterizing alterations at the level of the brain. However, we are extremely limited in our ability to acquire or experimentally manipulate human brain tissue from living patients or post-mortem brain slices. This has hampered efforts to study cellular and molecular abnormalities that accompany ASD, both during and after fetal and post-natal development. Notably, both the relative integrity of brain structures in affected individuals and the diversity of ASD genetics suggest that convergent mechanisms that contribute to affectation in ASD may operate at the level of the cell (3, 4). These may be identifiable in experimental models derived from affected individuals. In particular, ASD appears to frequently involve abnormal development and/or function of two major classes of neurons in the cerebral cortex, glutamatergic excitatory projection neurons (cExNs) and GABAergic inhibitory interneurons (cINs) (3, 5, 6). *In vitro* differentiation-based models of these neuronal cell types can identify cellular and molecular deficits associated with ASD, and provide a tractable platform to screen for pharmacologic agents that can rescue these deficits.

In recent years, such cellular models of ASD have been generated either by deriving induced pluripotent stem cell lines (iPSCs) from affected individuals or by using CRISPR/Cas9-based gene editing to engineer ASD-associated mutations into wild type PSCs (7-19). Most of these studies have focused on syndromic forms of ASD, or on monogenic, *de novo* cases, where causality is attributed to mutation of a single ASD-linked gene (10, 11, 13-16). These forms of ASD are attractive for cellular modeling, as they streamline study design and reduce many potential confounding variables. Other studies have included individuals with an unknown genetic cause of ASD, but with subject selection based upon a shared phenotypic characteristic, such as macrocephaly (18-20). Together, these models have been informative, revealing both

89 cellular and molecular alterations associated with affectation. These include shared and model-
90 specific disruptions of gene expression in ASD-derived neurons, frequently involving altered
91 expression of genes in key developmental signaling pathways, and genes that control cellular
92 proliferation and growth (7, 8, 13-20). In addition, differences were observed in neural precursor
93 cell (NPC) proliferation and differentiation (9, 19), neurogenesis, (9, 11, 18, 20), synaptogenesis
94 (8, 10, 17, 18), or functional neuronal activity (7-9, 11, 16, 17). Altered expression of ASD
95 genes, in which a mutation is linked to ASD causation or risk, is also frequently observed (7, 8,
96 13-16, 18-20).

97 These cellular modeling studies have revealed potential contributors to affectation and,
98 in some cases, have identified targets amenable to pharmacological rescue *in vitro* (10, 18).
99 However, they do not encompass the range of contributors to ASD burden in the general
100 population: no single gene mutation accounts for more than 1% of overall ASD cases with
101 predicted monogenic causality (21), while the majority of genetic risk appears to be polygenic or
102 idiopathic (2, 22-28). Polygenic ASD risk can involve both common and rare variation in protein-
103 coding and non-coding regions of the genome, which may act in a combinatorial manner (2, 27,
104 29, 30). Furthermore, ASD exhibits pronounced heritability in families (estimated at 50-90%
105 (31)), none of which can be accounted for by *de novo* (germline) events. Even within each
106 multiplex ASD family, there is often a considerable range in the extent of affectation among
107 individuals, and in most multiplex autism families, a single causative gene mutation usually
108 cannot be identified (31).

109 While ASD burden in the general population predominantly involves polygenic or
110 idiopathic risk, heritability, and variable affectation (2, 21, 27, 29-31), these genetically complex
111 forms of the disorder have been largely neglected in cellular modeling studies. Therefore, we
112 deemed it important to determine whether cellular modeling of these complex but prevalent
113 forms of ASD could also reveal affectation-related deficits. To test this, we focused on a

114 multiplex ASD family with variable affectation among family members. We generated iPSC lines
115 from three first degree relatives (a male and a female with differing degrees of affectation and
116 their unaffected mother) as well as an unrelated unaffected female. We used these lines to
117 perform differentiation into both cExN and cIN neural progenitors and/or neurons. Models from
118 the affected individuals exhibited compromised cellular responses to differentiation cues and
119 had disrupted gene expression profiles. This included altered expression of many ASD genes,
120 genes with roles related to behavior, cognition, and learning, and genes involved in nervous
121 system development and function, including cell adhesion molecules and ion channels.

122 This is, to our knowledge, the first cellular modeling study of multiplex ASD, including
123 graded affectation among family members. We demonstrated that even genetically complex
124 forms of ASD have discernable cellular and molecular abnormalities that track with affectation,
125 some of which overlap those identified in prior modeling of syndromic, monogenic, and *de novo*
126 forms of ASD. Therefore, this novel study design highlights the potential for cellular modeling to
127 identify convergent hallmarks across the broad diversity and genetic complexity of pathways to
128 affectation.

129 **Methods**

130 **Phenotyping of the Multiplex Family**

131 The nuclear family consisted of working professional non-consanguineous parents, whose first
132 born child was a daughter with DSM-5 Autism Spectrum Disorder (ASD), Level I (requiring
133 support, meeting DSM-5 criteria for Asperger Syndrome) who was very high functioning and
134 ultimately attended college, followed by a pair of monozygotic twin boys with ASD, Level III—
135 one more fluently verbal than the other but both severely impaired and requiring very substantial
136 support (see below)—followed by a third son with very subtle autistic traits and predominantly
137 affected by Attention Deficit Hyperactivity Disorder which improved substantially with stimulant

138 medication treatment. Trio Exome sequencing (ES) of one of the twins and his parents revealed
139 a variant of unknown significance (VUS) in *GPD2*, which was inherited by all of the children from
140 the mother, who is of above average intelligence with no dysmorphism and no history of
141 developmental problems. All pregnancies were uncomplicated, except for the post-natal hospital
142 course of the twins.

143 The daughter was born at term with no complications or dysmorphia. Her language and
144 motor development were typical and she was able to read at an early age. By age five she was
145 reading at a fifth-grade level. She has been described as talented in writing and drawing.
146 According to her parents, she exhibited social oddities from an early age, mainly in
147 communication, and has somewhat intense/restricted interests in fantasy games. She has
148 strong language abilities, and currently attends a four-year college, but at times uses odd
149 phrases and the rhythm of her speech includes irregular pauses. She has described feeling
150 alienated and "different", and was the victim of bullying in middle school, with few close friends.
151 In late adolescence, she developed major depressive disorder with moderate severity, which
152 brought her to first psychiatric contact. She is cognizant of some degree of social awkwardness,
153 which leads to feelings of anxiety and self-consciousness. The social anxiety inhibits her from
154 activities such as eating in the cafeteria and pursuing job opportunities for which she is
155 otherwise well-qualified. She has a history of becoming emotionally dysregulated and
156 overwhelmed in times of stress, which has led to self-injurious behaviors. She has had ongoing
157 struggles with depressive decompensation and suicidal ideation. She has above average
158 intelligence but has struggled academically in college due to depression and anxiety. She is
159 medically healthy with the exception of supraventricular tachycardia secondary to
160 atrioventricular node reentry, which was treated with ablation and resulted in subsequent
161 normalization of her electrocardiogram.

162 The twin boys were born at 35 weeks, had breathing problems at birth, and spent ten
163 days in the newborn intensive care unit. Neither child has any dysmorphic features or congenital
164 medical abnormalities, and brain imaging studies were negative. Likewise, neither child has a
165 history of confirmed seizures, however, there are concerns for possible absence epilepsy. There
166 is no history of abnormal neurological examination or macro-/microcephaly. Development of
167 both siblings was delayed, but neither had appreciable regression. The more severely affected
168 twin (designated as the affected proband, AP, and from whom the incuced pluripotent stem cell
169 (iPSC) model of severe ASD affectation was acquired) began to exhibit delays in development
170 by nine months of age. He was speaking single words at 14 months and was ultimately
171 diagnosed with autism at 3.5 years old. Research confirmation of the diagnosis was obtained
172 using the Autism Diagnostic Observation Schedule. Compared to his twin brother, he has had
173 more perseverative interests on odd objects. Psychological testing at the age of nine revealed
174 an IQ of 65 using the Leiter International Performance Scale. Now in late adolescence, he has
175 the ability to engage in reciprocal and meaningful verbal exchanges, although his language is
176 often echolalic and repetitive. He is socially motivated and develops superficial friendships with
177 peers. Functionally, he is able to complete most self-care, dress himself, prepare food and feed
178 himself, and count money. He participates in a vocational program at school and is able to
179 complete rudimentary tasks assigned to him. His monozygotic twin was also diagnosed with
180 ASD at 3.5 years old and is less severely affected, but still requires significant support. Selected
181 clinical characteristics of the family members studied are summarized in Table 1.

182 **Genotyping of the Multiplex Family**

183 Trio ES was performed by GeneDx for the unaffected mother (UM), the AP, and the unaffected
184 father. Briefly, sequencing was performed on an Illumina platform and reads were aligned to
185 human genome build GRCh37/hg19 and analyzed using Xome Analyzer, as described (32).
186 Mutation-specific testing was also performed by GeneDx on the intermediate phenotype sister

187 (IS) and the third trait-affected brother (TB) to confirm presence of the identified *GPD2* variant in
188 these individuals.

189 **iPSC generation**

190 iPSC lines were generated by the Genome Engineering and iPSC Center at Washington
191 University. Briefly, renal epithelial cells were isolated and cultured from fresh urine samples and
192 were reprogrammed using a CytoTune-iPS 2.0 Sendai Reprogramming kit (Thermo Fisher
193 Scientific), following the manufacturer's instructions. iPSC clones were then picked, expanded,
194 and characterized for pluripotency by immunocytochemistry (ICC) and RT-qPCR. At least three
195 clonal iPSC lines were derived for each subject and two different clones were used for
196 experimentation.

197 **iPSC maintenance and differentiation**

198 iPSC lines were grown under feeder-free conditions on Matrigel (Corning) in mTeSR1
199 (STEMCELL Technologies). cExN and cIN differentiation of iPSCs was performed using
200 previously described protocols (33). Briefly, for cExN differentiation, iPSCs were dissociated to
201 single cells with Accutase (Life Technologies) and 40,000 cells were seeded in V-bottom 96-well
202 non-adherent plates (Corning). Plates were spun at 200xg for five minutes to generate embryoid
203 bodies (EBs) and were incubated in 5% CO_2 at 37°C in cExN differentiation medium with 10μM
204 Y-27632 (Tocris Biosciences). cExN differentiation medium components include Neurobasal-A
205 (Life Technologies), 1X B-27 supplement (without Vitamin A) (Life Technologies), 10μM SB-
206 431542 (Tocris Biosciences), 100nM LDN-193189 (Tocris Biosciences). On day four of
207 differentiation, EBs were transferred from V-bottom plates to Poly-L-Ornithine- (20μg/ml) and
208 laminin- (10μg/ml) coated plates. Media (without Y-27632) was replenished every other day,
209 and on day 12 Neural Rosette Selection reagent (STEMCELL Technologies) was used to select
210 neural progenitor cells (NPCs) from within neural rosettes, per the manufacturer's instructions.

211 cExN NPCs were grown as a monolayer using cExN differentiation media for up to 15
212 passages. cIN differentiation media contained the same components as cExN differentiation
213 media, while also including 1μM Purmorphamine (Calbiochem) and 2μM XAV-939 (Tocris
214 Biosciences). EBs were generated as described for cExNs. At day four of differentiation, the
215 EBs were transferred to non-adherent plates and were placed on an orbital shaker (80 rpm) in
216 an incubator with 5% CO_2 at 37°C. The media was replenished every other day and, at day ten,
217 EBs were transferred to Matrigel- and laminin- (5μg/ml) coated plates. Y-27632 was included in
218 media until day eight of differentiation. On day 12 of differentiation, NPCs were dissociated with
219 Accutase and maintained as a monolayer for up to 15 passages. For both cIN and cExN NPC
220 growth analysis, an equal number of cells were seeded on Matrigel- and laminin- (5μg/ml)
221 coated plates and total cells were counted four days later when the cells reached 70-80%
222 confluence.

223 For differentiation of cExN NPCs into neurons for maturation, 40,000 cells per well were
224 seeded in V-bottom 96-well non-adherent plates. Plates were spun at 200xg for five minutes
225 and incubated in 5% CO_2 at 37°C in maturation medium with Y-27632. Maturation medium
226 components include Neurobasal-A, 1X B-27 supplement (without Vitamin A), 200μM cAMP
227 (Sigma), 200μM Ascorbic acid (Sigma), and 20ng BDNF (Tocris Biosciences). After two days,
228 EBs were transferred to Matrigel- and laminin- (5μg/ml) coated plates and media was
229 replenished every other day (without Y-27632). On day 12 of neuronal differentiation and
230 maturation, cells were dissociated with Accutase and seeded in an eight-well chamber for ICC.

231 For neurosphere size measurement analysis, p-values: $^{*}P<0.05$, $^{**}P<0.01$, $^{***}P<0.001$
232 were determined by a two-tailed Student's t-test.

233 **Sanger Sequencing**

234 DNA was isolated from cell lines using the PureLink Genomic DNA Kit (Invitrogen). Primers
235 were designed to amplify a 248 base pair region of *GPD2* flanking the identified point mutation
236 (forward primer: AAGCAGCAGACTGCATTTCA, reverse primer:
237 CACCATGGCACACACTTACC). Sanger sequencing was performed on this PCR amplified
238 fragment using either the forward or reverse primer. CodonCode Aligner software was used to
239 analyze sequencing results.

240 **Immunocytochemistry (ICC) and Immunoblotting**

241 For ICC, cells were plated on eight-well chamber slides coated with Matrigel and laminin (5
242 µg/mL). After one day, cells were washed once with PBS without calcium and magnesium (PBS
243 - Ca^{2+}/Mg^{2+}) and fixed in 4% Paraformaldehyde for 20 minutes, followed by washing with PBS +
244 Ca^{2+}/Mg^{2+}. Cells were blocked with blocking buffer (10% donkey serum, 1% BSA, and 0.1%
245 TritonX-100 in PBS + Ca^{2+}/Mg^{2+}) for at least one hour and incubated with primary antibodies
246 overnight (Additional file 1: Table S1) in antibody dilution buffer (1% donkey serum, 1% BSA,
247 and 0.1% TritonX-100 in PBS +Ca^{2+}/Mg^{2+}). After overnight incubation, cells were washed three
248 times with wash buffer (0.1% Triton X-100 in PBS + Ca^{2+}/Mg^{2+}). Cells were incubated with
249 corresponding secondary antibodies (Additional file 1: Table S1), along with DAPI (1mg/mL;
250 ThermoFisher Scientific), diluted in antibody dilution buffer for one hour. Following secondary
251 antibody incubation, cells were washed twice with wash buffer and once with PBS + Ca^{2+}/Mg^{2+}.
252 Slides were mounted with Prolong Gold anti-fade agent (Life Technologies). Images were
253 obtained using a spinning-disk confocal microscope (Quorum) with MetaMorph software and
254 were processed using ImageJ. For immunoblotting, cell lysate was extracted and 30µg of
255 protein was used per lane. Antibodies used are listed in Additional file 1: Table S1.

256 **FACS analysis**

257 For each experiment, approximately one million cells were pelleted, washed with PBS –
258 Ca^{2+}/Mg^{2+}, resuspended in PBS – Ca^{2+}/Mg^{2+} and fixed by adding 70% ice-cold ethanol dropwise
259 while vortexing. Cells were stained with 10ug/mL propidium iodide (Sigma) and 200ug/mL
260 RNase A (Fisher Scientific) in FACS buffer (PBS – Ca^{2+}/Mg^{2+}, 0.2% BSA, 1mM EDTA). FACS
261 was performed on single-cell suspensions and the cell cycle analysis function of FlowJo was
262 used to analyze cell cycle composition for each sample, based on propidium iodide staining to
263 detect DNA content in each cell. p-values: *P<0.05, **P<0.01, ***P<0.001 were determined by a
264 two-tailed Student's t-test.

265 **RNA-Seq and RT-qPCR**

266 Total RNA was collected from iPSC-derived day 12 cExN and cIN NPCs using the NucleoSpin
267 RNA II kit (Takara) per the manufacturer's instructions. RNA was quantified using a NanoDrop
268 ND-1000 spectrophotometer (Thermo Scientific), and the integrity of RNA was confirmed with
269 an Agilent Bioanalyzer 2100 to ensure a RIN value above eight. RNA-sequencing (RNA-seq)
270 library preparation and Illumina sequencing were performed by the Genome Technology Access
271 Center at Washington University. For RT-qPCR, 1µg total RNA was reverse transcribed using
272 iScript Reverse Transcription Supermix (Bio-Rad). Equal quantities of cDNA were used as a
273 template for RT-qPCR, using the Applied Biosystems Fast Real-Time quantitative PCR system.
274 RPL30 mRNA levels were used as endogenous controls for normalization. p-values: *P<0.05,
275 **P<0.01, ***P<0.001 were determined by a two-tailed Student's t-test.

276 **Bioinformatics and IPA analyses**

277 RNA-seq data analysis was performed as described in (33) to curate differentially expressed
278 gene (DEG) lists. To uncover the biological significance of DEGs, network analysis was
279 performed with the data interpretation tool Ingenuity Pathway Analysis (IPA) (Qiagen). IPA's
280 Ingenuity Knowledge Base uses network-eligible DEGs to generate networks and to define

281 connections between one or more networks. Based on the number of eligible DEGs, IPA
282 defines network scores as inversely proportional to the probability of finding the network and
283 defines significant networks (p≤0.001). Within each network, red symbols indicate upregulated
284 genes and green symbols indicate downregulated genes, where the color intensity represents
285 relative degree of differential expression.

286 **Results**

287 **Phenotyping and genotyping of the multiplex family**

288 The multiplex Autism Spectrum Disorder (ASD) pedigree selected for study (Fig. 1; Table 1)
289 underwent clinical phenotyping and genotyping (see Methods). From this pedigree, the
290 individuals selected for iPSC line derivation and modeling included the affected proband (AP),
291 his sister, who has an intermediate phenotype (IS), and their unaffected mother (UM) (indicated
292 in Fig. 1). As described above, a non-synonymous single nucleotide variant in the *GPD2* gene
293 was identified in the UM and all of the children (chr2:157352686 (hg19) G>A, NM_001083112.2
294 c.233G>A, p.G78E). This variant is not present in the father. The variant is in exon three of the
295 *GPD2* gene, within the region encoding the flavin adenine dinucleotide (FAD)-binding domain of
296 the GPD2 protein (Additional file 2: Fig. S1A). The GeneDx interpretation of this variant states
297 that it was not observed in approximately 6,500 individuals of European and African American
298 ancestry in the NHLBI Exome Sequencing Project and that it is evolutionarily conserved. In
299 addition, *in silico* analysis predicts that this variant is probably damaging to the protein structure
300 and function. Overall, GeneDx designated this as a variant of uncertain significance (VUS)
301 following the American College of Medical Genetics criteria. Subsequent mutation-specific
302 testing and Sanger sequencing identified this same variant in the AP, IS and trait-affected
303 brother (TB), while absent in an unrelated, unaffected control (UC) (Additional file 2: Fig. S1B).
304 Given the differential affectation of members of this pedigree carrying this variant, it was

305 apparent that this inherited VUS was insufficient to cause ASD by itself, but may have
306 contributed to polygenic risk/liability in this family.

307 **Generation of subject-derived iPSC models and directed differentiation into cortical**
308 **excitatory neurons**

309 Multiple clonal iPSC lines were derived from the UM, IS, and AP, and were characterized in
310 parallel with a single, clonal iPSC line derived from the UC. When grown in stem cell
311 maintenance media, there were no observable differences in expression of pluripotency
312 markers between these iPSC lines, as assessed by RT-qPCR (Additional file 2: Fig. S1C) and
313 immunocytochemistry (ICC) (Additional file 2: Fig. S1D). In addition, no differences in GPD2
314 protein levels were detected in iPSCs by ICC (Additional file 2: Fig. S1D) or Western blotting
315 (Additional file 2: Fig. S1E). Finally, we used FACS analysis of propidium iodide (PI)-stained
316 iPSCs to assess cell cycle progression and detected no observable differences between these
317 iPSC lines, which had similar percentages of cells in each stage of the cell cycle (Additional file
318 2: Fig. S1F-G).

319 In the cortex, as a result of their abnormal development, imbalances in glutamatergic
320 excitatory neurons (cExN) and GABAergic inhibitory interneurons (cINs) are thought to
321 contribute to neurodevelopmental disorders including ASD (3, 5, 34). We therefore differentiated
322 iPSCs derived from the UC, and from three family members (the UM, IS and AP), in parallel into
323 either cExN or cIN neural progenitor cells (NPCs) and/or neurons, to determine if we observed
324 any alterations in the *in vitro* development of either or both of these neural cell types. We
325 performed 12 days of cExN differentiation (four days as embryoid bodies (EBs) in V-bottom
326 plates, followed by eight days with the EBs plated for two-dimensional (2-D) culture; Fig. 2A). At
327 all time points assessed during this differentiation, the IS and AP lines generated significantly

328 smaller neurospheres than the UC and UM. The UM neurospheres were also slightly smaller
329 than those of the UC (Fig. 2B-C).

330 To identify whether an increase in apoptosis and/or a decrease in proliferation could be
331 contributing to these differences in neurosphere size, we performed FACS analysis of PI-
332 stained cells at day four of differentiation and found that the IS and AP neurospheres had a
333 significantly higher fraction of sub-G1 (apoptotic) cells, compared to neurospheres derived from
334 the UM and UC lines (<2N DNA content; Fig. 2D-E, G). There was a corresponding decrease in
335 the percentage of cells in the G1 phase of the cell cycle in the IS and AP neurospheres (2N
336 DNA content; Fig. 2D, F-G). However, neurospheres from all lines had similar percentages of
337 cells in the S and G2/M phases of the cell cycle, suggesting that their cell cycle characteristics
338 and rates of progression were otherwise similar (S phase and 4N DNA content; Fig. 2D, G). To
339 determine whether induction of neural differentiation was a stressor that was contributing to this
340 increase in apoptosis in the IS and AP line-derived neurospheres, we compared sphere size
341 after culturing spheres from each line either in stem cell maintenance media (mTeSR) or in
342 neural induction media. In general, sphere size was larger for all cell lines when kept in mTeSR
343 media rather than neural induction media, while the differences in sphere size for the IS and AP
344 versus the UC and UM was much less pronounced in mTeSR relative to differences seen under
345 neural induction conditions (Fig. 2H-I). These data suggest that, by comparison with the UC and
346 UM, the IS and AP lines have a slightly elevated propensity to undergo apoptosis upon
347 dissociation and sphere formation, while this is exacerbated by induction of neural
348 differentiation.

349 We next maintained these four lines as NPCs after neural rosette selection at day 12
350 and then subjected them to PI staining and FACS analysis. Unlike the results from earlier time
351 points, the cExN NPCs showed no significant differences in cell cycle across the four lines
352 (Additional file 2: Fig. S2A-B), nor in the rate of growth/death over the course of culture for four

353 days (Additional file 2: Fig. S2C). However, morphological analysis by bright field imaging
354 indicated a possible adhesion defect in the IS NPCs, as indicated by uneven growth on the cell
355 culture plate surface (Additional file 2: Fig. S2D). At the NPC stage, GPD2 protein levels
356 remained similar across the four lines, as was shown for iPSCs (Additional file 2: Fig. S2E).

357 Finally, to determine if the NPCs derived from the affected individuals exhibited an
358 altered capacity to differentiate into cExN neurons, NPCs from the four lines were further
359 differentiated for 12 days as shown (Additional file 2: Fig. S3A) and subjected to ICC. No
360 apparent differences between the four lines were observed in the expression of NPC markers
361 (PAX6, NESTIN, and SOX1) or markers of immature (TUJ1) and mature cExN neurons
362 (VGLUT, MAP2) (Additional file 2: Fig. S3B). Furthermore, there were no observable differences
363 between the lines in the fraction of cells expressing Ki-67, a marker of cell proliferation, or
364 cleaved Caspase-3, a marker of apoptosis (Additional file 2: Fig. S3B).

365 **Differentiation of subject-derived iPSCs into cortical interneuron progenitors**

366 We also characterized cellular phenotypes of these four lines during differentiation into cIN
367 NPCs, to determine any differences between the development of this neural cell type in lines
368 derived from affected versus unaffected individuals. The differentiation scheme to produce cIN
369 NPCs is outlined in Figure 3A. On day five of differentiation in this scheme, neurospheres
370 derived from the IS line were smaller than those of the UM. Conversely, the AP line-derived
371 neurospheres were slightly larger than the UM line neurospheres (Fig. 3B-C).

372 After dissociation on day 12 of differentiation, we assessed the cell cycle of the cIN
373 NPCs using FACS of PI-stained cells. The IS and AP cIN NPCs had an increased sub-G1 cell
374 population, compared to the UC and UM NPCs, an indication of increased apoptosis in the cells
375 from the affected individuals (Fig. 3D). Correspondingly, there was a decrease in the proportion
376 of cells in the G1 phase of the cell cycle (Fig. 3E-F). However, no differences were observed in

377 frequencies of cells in the S and G2 phases of the cell cycle between lines, suggesting that
378 these lines had similar proliferation rates (Additional file 2: Fig. S2F). This result was supported
379 by analysis of NPC cell counts after four days of growth, which revealed a significant reduction
380 in the number of AP NPCs, as well as a slight reduction in the number of IS NPCs, compared to
381 the UM NPCs (Additional file 2: Fig. S2G). These reductions in NPC number may result from the
382 increased NPC apoptosis detected in our PI FACS analysis. The AP NPCs also exhibited
383 altered morphology that could indicate impaired adhesion capacity relative to the control UM/UC
384 lines, which could also contribute to the reduction in the number of AP NPCs persisting in the
385 culture after four days of growth (Additional file 2: Fig. S2H).

386 **Transcriptomic differences in neural progenitor cells derived from affected individuals**
387 **versus controls**

388 To investigate which classes of genes could be differentially expressed in neural cells from the
389 affected individuals, by comparison with the unaffected controls, we performed RNA-seq
390 analysis on both cExN and cIN NPCs at day 12 of differentiation for all four subject-derived
391 lines. Four biological replicates were analyzed for each sample type and were clustered by
392 principal component analysis (PCA) of processed reads (Additional file 2: Fig. S4A-B). We
393 defined genes that were significantly differentially expressed genes (DEGs) in pairwise
394 comparisons of these four sample types for either cExN or cIN NPCs, selecting DEGs with a p-
395 value of <0.05 and a fold difference between sample types of >2 (Additional file 3: Table S2). In
396 a within-family comparison of the UM, IS, and AP samples, greater numbers of DEGs were
397 obtained in the cIN NPC pairwise comparisons, versus the numbers of DEGs obtained for cExN
398 NPC pairwise comparisons (Additional file 2: Fig. S4C-D). These data indicate that the cIN
399 samples from the affected individuals (IS/AP) exhibit more transcriptomic differences from the
400 UM control than the affected individual-derived cExN samples.

401 We focused first on identifying classes of genes that were differentially expressed in
402 NPCs derived from the affected individuals, by comparison with unaffected controls. To do this,
403 we defined the subset of DEGs that were similarly expressed in samples from both affected
404 individuals (AP/IS) but that differed in expression by comparison with the unaffected mother
405 (UM) sample. Relative expression is also shown for the UC, for a full cross-sample comparison.
406 452 and 437 DEGs for the cExN and cIN NPC samples met these criteria, respectively.
407 Hierarchical clustering and visualization of the relative expression of these DEGs across the
408 four sample types is shown for the cExN NPCs (Fig. 4A, Additional file 4: Table S3). We next
409 used Ingenuity Pathway Analysis (IPA) to assess the potential biological significance of these
410 genes. For the 452 DEGs in the cExN NPCs described above, the most significant function- and
411 disease-related gene ontology (GO) terms included 'behavior', 'neurological disease', and
412 'embryonic development' (Fig. 4B). Network analysis using IPA revealed several interesting
413 networks of DEGs related to these GO terms, including networks related to 'locomotion' (from
414 DEGs within the 'behavior' GO term) and 'behavior and developmental disorder' (Fig. 4C-D).
415 Within the 'locomotion' network, most genes were upregulated in the affected individuals
416 compared to the controls, including genes relating to neural adhesion and ion channels (Fig. 4C
417 and Additional file 5: Table S4). Genes with known roles in NPCs or neurons, as well as stress-
418 related genes were present in the larger 'behavior and developmental disorder' network (Fig. 4D
419 and Additional file 5: Table S4). Interestingly, another network comprising genes from the GO
420 term 'neurological disease' is related to 'inflammation of central nervous system' (Additional file
421 2: Fig. S5A and Additional file 5: Table S4).

422 IPA analysis of the cIN DEGs also revealed several interesting classes of genes that
423 were differentially expressed between the affected participants and unaffected control NPC-
424 derived samples. Hierarchical clustering and visualization of the relative expression of DEGs
425 across the four sample types for the cIN NPCs is shown in Fig. 4E (Additional file 4: Table S3).

426 The top GO terms included ‘developmental disorder’, ‘behavior’, ‘nervous system development
427 and function’, ‘psychological disorders’, and ‘neurological disease’ (Fig. 4F). Within the term
428 ‘behavior’, a network that includes ‘learning’-, ‘cognition’-, and ‘behavior’-related genes was
429 identified (Fig. 4G, Additional file 5: Table S4). The network related to the GO term
430 ‘psychological disorder’ includes genes related to ‘anxiety disorders’, ‘mood disorders’, and
431 ‘depressive disorder’ (Fig. 4H). The ‘nervous system development and function’ network
432 includes genes involved in the ‘quantity of neurons’ and ‘quantity of synapse’, as well as cell
433 adhesion genes (Additional file 2: Fig. S5B and Additional file 5: Table S4). Finally, a
434 ‘neurological’ network included a number of genes also present in the other networks (Additional
435 file 2: Fig. S5C). Taken together, this analysis of DEGs in both cExN and cIN NPCs shows
436 evidence of altered expression of a number of neurological and psychological disease-relevant
437 gene classes in the AP- and IS-derived lines, relative to lines derived from the UM and/or UC.

438 **Within-family comparison identifies a transcriptome signature specific to neural**
439 **progenitor cells derived from the ASD-affected proband**

440 As differences in genetic background can confound differential gene expression analysis (35),
441 we also performed a pairwise, within-family data comparison of DEGs that distinguish the UM-,
442 IS-, and AP-derived samples, focusing on DEGs specific to the AP that could contribute to the
443 greater degree of affectation observed. Using pairwise comparisons of DEGs, we defined 190
444 genes which were uniquely differentially expressed in cExN NPCs from the AP (Fig. 5A). The
445 top GO terms associated with these AP-specific DEGs included ‘psychological disorders’,
446 ‘behavior’, ‘nervous system development and function’, ‘developmental disorder’, and
447 ‘neurological disease’ terms (Fig. 5B). Within the ‘behavior’ term, network analysis showed
448 genes related to ‘memory’ and ‘learning’ to be dysregulated (Fig. 5C and Additional file 5: Table
449 S4). Within the ‘nervous system development and function’ term, a network of dysregulated
450 genes related to ‘differentiation of neurons’ was identified (Fig. 5D, Table S4).

451 Similar analysis was performed on the cIN samples, revealing 384 DEGs unique to the
452 AP samples in the within-family comparison (Fig. 5E). IPA analysis identified classes of DEGs
453 related to the GO terms 'psychological disorders', 'developmental disorder', 'neurological
454 disease', 'behavior', and 'nervous system development and function' (Fig. 5F). Within the
455 'behavior' disease term, a network of genes related to 'behavior' and 'cognition' was identified
456 (Fig. 5G and Additional file 5: Table S4). Within the 'nervous system development and function'
457 term, a network of genes related to 'development of neurons' and 'synaptic transmission' had
458 altered expression in the AP versus the IS/UM-derived samples (Fig. 5H and Additional file 5:
459 Table S4). Together, this analysis identifies AP-unique DEGs in both cExN and cIN NPCs,
460 many of which are broadly related to neural development, as well as to specific aspects of ASD,
461 such as behavioral alterations. These gene expression changes therefore correlate with and
462 may contribute to, the severity of affectation in the AP.

463 **Comparison of differentially expressed genes with ASD-associated genes and validation**

464 The Simons Foundation Autism Research Initiative (SFARI) (36) maintains a database of genes
465 that are mutated to cause, or contribute to, ASD risk. We compared our DEGs to these ASD
466 genes, to assess whether their dysregulated expression could contribute to affectation in these
467 individuals. Of 452 DEGs in the cExN differentiation scheme that had similar expression in the
468 AP and IS that differed from that seen in the UM, 30 (6.6%) were ASD genes (Fig. 6A). For the
469 corresponding cIN NPC comparison, 46 of 437 DEGs (10.5%) were ASD genes in the SFARI
470 Gene database (Fig. 6B). Based upon the 1019 genes present in the SFARI Gene database
471 (36) and the total of 27,731 genes with >0.1 RPKM average expression across all cExN and cIN
472 samples, the number of AP- and IS-specific DEGs that are AD genes is significantly greater
473 than would be expected by chance (hypergeometric distribution, $p=9.35x10^{-5}$ and $1.95X10^{-12}$ for
474 cExN and cIN data, respectively). Therefore, it is possible that misregulated expression and

475 consequently function of ASD genes contributed to disruption of neural development and/or
476 continues to contribute to altered neurological function in the IS and AP.

477 We validated the differential expression of a subset of the DEGs described above by RT-
478 qPCR analysis, isolating RNA from NPCs derived from a second set of iPSC clones that differed
479 from those used for the RNA-seq experiments. Expression changes of DEGs selected from the
480 cExN NPC RNA-seq data (Fig. 7A) were robustly recapitulated in these experiments (Fig. 7B).
481 Genes from the 'behavior and developmental disorder', from other identified networks, and
482 genes involved in neurodevelopment were evaluated (Additional file 5: Table S4). We also
483 derived cIN NPC RNA from a second set of iPSC clones and validated the corresponding RNA-
484 seq data for a subset of the DEGs (Fig. 7C). Differential expression was assessed for SFARI
485 ASD genes (36), and for genes encoding transcription factors, ion channels, and cell adhesion
486 molecules (Fig. 7D-E and Additional file 5: Table S4). In addition, we validated a subset of
487 DEGs in cINs which also had differential expression in cExN NPCs (Fig. 7E). Together, these
488 analyses revealed that, relative to unaffected individuals, samples from affected individuals
489 exhibited altered expression of classes of genes involved in behavior, learning, cognition, mood
490 disorders, and neurodevelopment, including perturbed ASD gene expression, suggesting that
491 these differences could contribute to aberrant neural development or function in the affected
492 individuals.

493 **Discussion**

494 In recent years, the genetic structure of Autism Spectrum Disorder (ASD) risk in the general
495 population has been clarified. This work has confirmed that while, in some cases, deleterious,
496 single gene variants are significant contributors to ASD, the vast proportion of population
497 attributable risk is polygenic (2, 37). Furthermore, this risk is highly heritable, and individuals
498 within a multiplex family typically exhibit variable degrees of affectation (31). Here, we modeled

499 cellular and molecular correlates of ASD within one such multiplex family, performing cortical
500 neural differentiation of iPSCs derived from several family members with differential affectation.
501 In this family, both polygenic liability and a shared variant of unknown significance (VUS) may
502 contribute to risk. In cells derived from the affected individuals, we identified compromised
503 responses to differentiation cues and altered gene expression profiles during iPSC
504 differentiation into cortical excitatory (cExN) and inhibitory (cINs) neurons, compared to related
505 and unrelated unaffected controls. This work demonstrates that iPSC-based modeling can be
506 used to characterize these more genetically complex but prevalent forms of ASD, in addition to
507 modeling simplex and monogenic forms, which have been the focus of most studies to date.
508 Moreover, these data provide information on physiologic and transcriptomic signatures of
509 multiplex autism, with which cellular models derived from other families and other combinations
510 of inherited susceptibility factors can be compared in future work.

511 Our phenotypic analysis of these four iPSC-based models of cortical neural development
512 included assays conducted in the stem cells, during neural specification, in the proliferating
513 NPCs, and during neuronal differentiation. During cExN NPC specification and during cIN NPC
514 propagation, models from both affected individuals exhibited elevated fractions of cells with sub-
515 G1 DNA content, relative to control-derived models. These data suggest that models derived
516 from the affected individuals are less resistant to stressors, such as induction of differentiation,
517 with these stressors increasing the propensity for cells to undergo apoptosis. While the
518 molecular trigger for the induction of apoptosis here is unclear, expression of stress and
519 apoptosis-related genes, such as *CHCHD2, ANXA1, and SPATA18* are dysregulated in these
520 models (38-42). These findings are reminiscent of some observations made in prior work, in
521 which schizophrenia subject-derived iPSCs exhibited reduced neurosphere size (43) and
522 increased apoptosis was observed in Williams-Syndrome iPSC-derived NPCs (44).
523 Interestingly, few studies report cellular alterations observed prior to the NPC stage, often

524 focusing predominantly on phenotypes seen in NPCs and mature neurons (7-19). While this
525 may reflect a lack of earlier phenotypic changes in some models, our findings highlight the
526 importance of tracking neurodevelopmental alterations from their earliest onset. A recent report
527 underscores the value of using cellular modeling approaches that aim to recapitulate some
528 aspects of *in vivo* neurodevelopment (20). This study found that direct conversion of iPSCs into
529 neurons masked ASD-associated cellular phenotypes, which were observable during directed
530 differentiation of iPSCs (20).

531 In our study, transcriptomic analysis of neural progenitor cells revealed dysregulated
532 expression in affected individuals compared to controls of gene networks related to behavior,
533 psychological disorders, and neuronal development and disease. Genes encoding transcription
534 factors were among the neurodevelopment-related genes with reduced expression in both
535 affected individuals. For example, ARX is required for normal telencephalic development and is
536 associated with syndromic autism and other neurodevelopmental disorders (45), while EMX1
537 and FOXB1 also play important roles in neural development (46-48). Behavioral misregulation is
538 a key trait of ASD, and gene networks related to the GO term 'behavior' exhibited dysregulated
539 expression in both affected individuals. Genes in these networks include *COMT, ADCYAP1,*
540 *CNR1, HTR2C, GRIK2,* and *RGS4*, all of which are implicated in behavior-related phenotypes in
541 humans and/or mice (49-57). ASD genes were also dysregulated in these affected individuals,
542 relative to controls. Mutation of these genes in other individuals is implicated in autism risk or
543 causation. These include adhesion-related genes (*PCDHA1*, *PCHDHA6*, *PCDHGA11, PCDH8,*
544 *PCDH9, PCDH10* (58-62)*, KIRREL3* (63), *CNTN3*, *CNTN*4 (64), *CNTNAP4* (65), and *THBS1*
545 (66)), receptor and channel genes (*CACNA2D3* and *SCN9A* (67)*, GRIK2* and *GRIK3* (68-71),
546 *KCNJ2* (72, 73)*,* and *GRIA1* (74, 75)), and genes associated with central nervous system
547 development and axon guidance (*ERBB4* (76, 77), *NTNG1* (78), *TSHZ3* (79), *EBF3* (80)*,*
548 *MYT1L* (81, 82), and *ANXA1* (40-42)). Altered expression of ASD-associated genes has also

549 been observed in cellular models derived from affected individuals in other studies (8, 13-16, 19,
550 83). Therefore, these findings suggest that misregulated expression of suites of ASD-associated
551 genes may contribute to risk or affectation, and may do so by altering neurodevelopment and/or
552 neuronal function in these affected individuals.

553 A unique aspect of this study is the use of iPSC-based directed differentiation into both
554 cExNs and cINs, enabling us to identify neural cell type-specific alterations associated with
555 affectation. Although DEGs identified in affected individuals in both neural cell types were
556 associated with many similar functions and diseases (e.g. behavior), the specific DEGs obtained
557 often varied by cell type. For example, cIN DEGs included many more ASD-associated genes
558 and protocadherin genes, the latter of which control neuronal migration, axonal growth, and
559 synapse formation (60, 61). Human post-mortem cortical tissue from individuals with ASD has
560 been shown to exhibit disrupted expression of cIN-associated genes, evidence that this cell type
561 may commonly be disrupted in affected individuals *in vivo* (84). These findings suggest that
562 extending cellular modeling studies to multiple disease-relevant neuronal cell types, including
563 cINs, may reveal additional neurodevelopmental disruptions related to affectation.

564 To define cellular and molecular perturbations commonly related to affectation, we
565 compared our findings to other studies that modeled ASD by directed differentiation of iPSCs
566 into cExNs. We identified subsets of overlapping DEGs in comparisons with studies involving
567 idiopathic autism cases vs. controls (26 shared DEGs; (7)), syndromic ASD involving
568 macrocephaly (31 shared DEGs; (19)), and modeling of the syndromic ASD gene *CHD8 (*32
569 shared DEGs*;* (13)) (Additional file 6: Table S5). Data for such comparisons is limited at present
570 because iPSC-based models have been generated for a relatively small number of individuals
571 and mutations, and these almost exclusively characterize cExNs or cerebral organoids (7, 13,
572 18, 19).

573 The multiplex pedigree studied here was subjected to clinical exome sequencing, as it was
574 hypothesized that a single, shared, genetic contributor might mediate autism risk and differential
575 phenotypic expression by sex in this family. In this sequencing analysis, a thread of shared
576 genetic liability amongst all children was a VUS in the ASD and ID-associated gene, *GPD2* (85-
577 87), which was inherited from their mother. However, there is variable ASD expressivity
578 amongst these individuals, ranging from absent, to intermediate, to severe. In addition, both
579 males and females in the pedigree are variably affected, indicating the presence of other
580 significant contributors to variation in severity of affectation within this family. This observation is
581 consistent with recent evidence that genetic liability for ASD is prevalently polygenic, and that,
582 even in multiplex pedigrees where a significant monogenic contributor has been identified,
583 additional polygenic risk can contribute to affectation (37). Moreover, this multiplex family was
584 prototypic in reflecting the most severe form of affectation occurring in a male.

585 We hypothesized that it might be possible to identify graded cellular phenotypes that
586 correlated with the level of severity of phenotypic expression. In general, we instead observed
587 many cellular and molecular alterations that were shared by the cellular models derived from the
588 affected individuals, while not being observed in those derived from the unaffected individuals.
589 However, we did define some proband-specific DEGs, not present in the less severely affected
590 sister, many of which relate to behavior and nervous system development. A subset of these
591 DEGs had graded expression, exhibiting intermediate expression levels in the intermediate
592 phenotype sister, between her unaffected mother and her severely affected brother. These
593 findings suggest that both the degree of dysregulation of expression and the number and
594 identity of DEGs within these networks may contribute to the level of affectation. While further
595 experimentation might reveal additional graded phenotypes, particularly in mature neurons, *ex*
596 *vivo* cellular modeling cannot recapitulate many aspects of fetal and post-natal

597 neurodevelopment that may have been perturbed to contribute to the graded affectation
598 observed in these individuals.

599 This work highlights several considerations for ongoing scientific efforts to model this
600 complex but prevalent form of ASD in future studies. First, since the unique characteristics of
601 any multiplex pedigree present challenges for cellular modeling, it is important to control for sex
602 and variation in affectation in subject and family selection, study design, and analysis. Related
603 to this point is the importance of modeling affected females in such studies. Most ASD cellular
604 modeling to date has been restricted to affected males (7-10, 13, 14, 16, 18, 19), given the
605 increased prevalence of ASD among males, and the fact that constraint to a single sex
606 simplifies some modeling considerations. In particular, sex chromosome dosage effects do not
607 need to be accounted for in male cells, while female-derived iPSC models cannot currently
608 recapitulate the process of random X-chromosome inactivation that occurs in developing
609 somatic tissues, including the brain (88, 89). Interestingly, the transcriptomic differences that we
610 observed here were not driven by sex-linked gene expression: very few DEGs in any potential
611 pairwise sample comparison (whether between same or opposite sex models) were sex
612 chromosome-linked potential contributors to sex-biased gene expression in the human brain
613 (90, 91). Therefore, this work supports the feasibility of identifying DEGs associated with
614 affectation by cellular model cross-comparisons, even when these models are derived from both
615 female and male subjects.

616 Another consideration for iPSC-based modeling of ASD is genetic background, which
617 can be a confounding variable for cross-comparisons (35). In this pedigree, ASD risk was
618 polygenic, such that it was not possible to engineer a correction of a single genome variant to
619 create pairs of isogenic mutant versus wild-type iPSC lines with an identical genetic background
620 for study. In such cases, modeling of first degree relatives may serve as the best control, and
621 modeling of multiple related individuals with varying affectation provides additional opportunities

622 for identifying potential contributors to these differences in affectation. Including unrelated
623 controls and performing comparisons with other studies can further highlight which phenotypic
624 and transcriptomic alterations track with affectation, even by comparison with models derived
625 from individuals with an unrelated genetic background.

626 **Conclusions**

627 In summary, this work used robust schemes for differentiation of cortical neurons from iPSCs to
628 model cellular and molecular signatures associated with multiplex ASD in a family reflecting
629 varying degrees of affectation. Even in this prevalent, complex form of ASD, involving
630 heritability, polygenic etiology, and variable affectation, we could identify affectation-linked
631 cellular and molecular alterations of neurodevelopment, some of which overlapped those
632 defined in other iPSC-based studies of monogenic, syndromic, and *de novo* ASD. As more
633 cellular models of ASD are characterized, these data can be harnessed in the search for
634 convergent and divergent contributors to impairment across the genetically complex and multi-
635 factorial pathways that give rise to ASD.

636 **Abbreviations**

637 ASD: Autism Spectrum Disorder; iPSCs: Induced Pluripotent Stem Cells; cExNs: Cortical
638 Excitatory Neurons; cINs: Cortical Inhibitory Neurons; NPCs: Neural Progenitor Cells; ES:
639 Exome Sequencing; UM: Unaffected Mother; AP: Affected Proband; IS: Intermediate Phenotype
640 Sister; UC: Unaffected Control; GTAC: Genome Technology Access Center; ICC:
641 Immunocytochemistry; RT-qPCR: quantitative reverse transcription PCR; EBs: Embryoid
642 Bodies; DEG: Differentially Expressed Gene; IPA: Ingenuity Pathway Analysis; VUS: Variant of
643 Unknown Significance; PI: Propidium Iodide; PCA: Principal Component Analysis; GO: Gene
644 Ontology; SFARI: Simons Foundation Autism Research Initiative.

645 **Ethics approval and consent to participate**

646 Subjects were consented for biobanking and iPSC line generation by the Washington University
647 Institutional Review Board of the Human Research Protection Office under human studies
648 protocol #201409091 (Dr. John Constantino).

649 **Consent for publication**

650 Consent to publish data was provided by all subjects.

651 **Availability of data and materials**

652 The RNA-seq data generated during the current study are available in the Gene Expression
653 Omnibus (GEO) repository as Series GSE129806. The ASD gene dataset analyzed during the
654 current study is available in the SFARI Gene database at https://gene.sfari.org.

655 **Competing interests**

656 The authors declare that they have no competing interests.

657 **Funding**

This project was supported by NIH/NICHD grant U54 HD087011 to JNC; NIH/NIGMS GM 66815, March of Dimes Grant 1-FY13-413, WUSM Institute for Clinical and Translational Sciences (ICTS) grant JIT-NOA_619 (from NIH/NCATS UL 1TR002345 to ICTS), and a grant from the McDonnell Center for Cellular and Molecular Neurobiology at WUSM to KLK; NIH/NIGMS T32 GM 7067-43, the Precision Medicine Pathway at WUSM, and the Irving Biome Graduate Student Fellowship at WUSM to EMAL; NIH K12 HL120002 to DB.

Author's contributions

E.M.A.L. contributed to the study design, carried out all cExN experimentation, analyzed data, and prepared the manuscript. K.M. contributed to the study design, carried out all cIN experimentation, analyzed data and contributed to manuscript preparation. D.B. interpreted clinical exome sequencing data and contributed to manuscript preparation. P.G. and B.Z. performed RNA-seq data analysis. A.B. contributed to the study design. J.N.C. contributed to the study design and manuscript preparation. K.L.K. contributed to the study design, data analysis, and manuscript preparation. All authors read and approved the final manuscript.

Acknowledgments

We thank the family for providing biomaterials for use in this study. We thank the Genome Engineering and iPSC Center (GEiC) at Washington University School of Medicine (WUSM) for deriving the iPSC lines used in this study. We thank the Alvin J. Siteman Cancer Center at WUSM, for the use of the Siteman Flow Cytometry Core, which provided self-service Flow Cytometry Analysis. The Siteman Cancer Center is supported in part by an NCI Cancer Center Support Grant #P30 CA091842. We thank the Genome Technology Access Center in the Department of Genetics at WUSM for providing genomic sequencing services. The Center is partially supported by NCI Cancer Center Support Grant #P30 CA91842 to the Siteman Cancer Center and by ICTS/CTSA Grant# UL1 TR000448 from NIH/NCRR.

682 **Figure Legends**

683 **Table 1. Selected clinical characteristics and mutational status of several individuals in**
684 **the multiplex ASD pedigree.**

685 **Figure 1**. **Pedigree from which samples were derived for this study.** *GPD2* mutational
686 status (GPD2m: indicates mutational status) and degree of ASD affectation are indicated. Black
687 shading corresponds to the affected proband (AP) and his twin brother, dark grey to the
688 intermediate phenotype sister (IS), light grey to the trait-affected brother (TB), and white to
689 unaffected family members, including the unaffected mother (UM). * indicates that renal
690 epithelial cells from these individuals were used to derive multiple, clonal iPSC lines.

691 **Figure 2**. **Characterization of iPSC lines during differentiation into cExN NPCs. (A)**
692 Differentiation scheme, including timeline and small molecules used. **(B-C)** iPSCs derived from
693 an unrelated, unaffected control (UC), as well as the UM, IS, and AP were differentiated for 12
694 days to generate cExN NPCs. Neurosphere size at several time points is shown in (B) and
695 quantified in (C) (mean±SEM; scale bar = 500μm; n=12 biological replicates, encompassing two
696 different clonal lines from each subject, and one clonal line for the UC). **(D-G)** At day four of
697 differentiation, cells were stained with propidium iodide and FACS analysis of DNA content was
698 performed. (D) Representative FACS plots. In (E) <2N (sub-G1) and (F) 2N (G1) cells are
699 quantified, with values shown for each replicate. (G) shows mean values for all cell cycle stages
700 for each cell line (mean±SEM; n≥3 biological replicates for each subject, encompassing two
701 different clonal lines from each subject, and one clonal line for the UC). **(H-I)** iPSCs were
702 differentiated in either induction media or mTeSR stem cell media, and EB size was analyzed at
703 day four of differentiation. Representative images are shown in (H) (scale bar = 500μm), with
704 quantification in (I) (n=3 biological replicates from one clonal line for each subject). p-values:

705 *P<0.05, **P<0.01, ***P<0.001 were determined by a two-tailed Student's t-test and all other
706 pairwise comparisons had a non-signficant p-value (P≥0.05).

707 **Figure 3**. **Characterization of iPSC lines during differentiation into cIN NPCs. (A)**
708 Differentiation scheme, including timeline and small molecules used. **(B-C)** iPSCs were
709 differentiated for 12 days to obtain cIN NPCs, with differences in neurosphere size shown in (B)
710 and quantified in (C) (mean±SEM; scale bar = 250μm; n=3 biological replicates from one clonal
711 line for each subject). **(D-F)** NPCs were stained with propidium iodide and analyzed by FACS
712 for DNA content. In D and E, respectively, <2N (sub-G1) and 2N (G1) cells were quantified, with
713 values shown for each replicate (n=3 biological replicates from one clonal line for each subject).
714 (F) shows representative FACS plots. p-values: *P<0.05, **P<0.01, ***P<0.001 were
715 determined by a two-tailed Student's t-test and all other pairwise comparisons had a non-
716 signficant p-value (P≥0.05).

717 **Figure 4**. **Transcriptomic analysis of genes with differential expression in affected**
718 **subject-derived NPCs, relative to unaffected controls. (A)** Hierarchical clustering of RNA-
719 seq data from the cExN NPCs identified differentially expressed genes (DEGs) with shared
720 expression in the AP and IS that differed from that in the UM. Relative expression is also shown
721 for the UC, for a full cross-sample comparison (p<0.05, fold-change >2; n=4 biological replicates
722 from one clonal line for each subject). **(B-D)** Ingenuity Pathway Analysis (IPA) of these cExN
723 NPC DEGs defined disease and function-associated gene ontology (GO) terms and identified
724 gene networks associated with the (C) 'behavior' (D) and 'behavior and developmental disorder'
725 GO terms. **(E)** Hierarchical clustering of RNA-seq data for the cIN NPCs identified DEGs with
726 shared expression in the AP and IS, that differed from that in the UM. Relative expression is
727 also shown for the UC, for a full cross-sample comparison (p<0.05, fold-change >2; n=4
728 biological replicates from one clonal line for each subject). **(F-H)** IPA analysis of these cIN NPC
729 DEGs defined (F) disease- and function-associated GO terms and identified gene networks

730 associated with (G) 'behavior' and (H) 'psychological disorder'. Within each network, red
731 symbols indicate upregulated genes and green symbols indicate downregulated genes, while
732 color intensity indicates relative degree of differential expression.

733 **Figure 5. Within-family analysis of transcriptomic signatures specific to the affected**
734 **proband-derived samples. (A)** Venn diagram for the cExN NPCs, showing the DEGs from
735 pairwise comparisons of different samples, including numbers of overlapping DEGs. The blue
736 shaded portion of the Venn diagram indicates DEGs unique to the AP, not shared by the IS or
737 UM. **(B-D)** Ingenuity Pathway Analysis (IPA) of the AP-unique DEGs in cExN NPCs defined
738 class and function-associated GO terms (B) and identified gene networks associated with
739 'behavior' (C) and 'nervous system development and function' (D). **(E-H)** IPA analysis of the AP-
740 unique DEGs in cIN NPCs determined (F) class and function-associated GO terms and
741 identified gene networks associated with (G) 'behavior' and (H) 'nervous system development
742 and function'. Within each network, red symbols indicate upregulated genes and green symbols
743 indicate downregulated genes, where the color intensity represents relative degree of differential
744 expression.

745 **Figure 6**. **Hierarchical clustering of DEGs that are also ASD genes in the SFARI autism**
746 **gene database**. **(A)** Relative gene expression for the cExN NPC samples. **(B)** Relative gene
747 expression for the cIN NPC samples. Data from four biological replicates are shown for each
748 sample type.

749 **Figure 7. Validation of DEGs of interest identified from RNA-seq experiments by RT-**
750 **qPCR.** Genes tested are related to behavior and developmental disorders, adhesion, and ion
751 channels. **(A-B)** Comparison of relative gene expression in cExN NPCs for the UM, IS, and AP
752 by (A) RNA-seq and (B) RT-qPCR, including expression analysis of genes related to 'behavior
753 and developmental disorders'. **(C-E)** Comparison of gene expression between the UM, IS and

754 AP for the cIN NPCs by (C) RNA-seq and by (D-E) RT-qPCR, both for genes that were (D)
755 differentially expressed only in the cIN NPCs and (E) for genes that were differentially
756 expressed in both cExN and cIN NPCs. p-values: *P<0.05, **P<0.01, ***P<0.001 were
757 determined by a two-tailed Student's t-test and all other pairwise comparisons had a non-
758 signficant p-value (P≥0.05). RT-qPCR data shown includes n≥3 biological replicates from one
759 clonal line per subject, where samples were generated for each subject by using a second
760 clonal iPSC line that differed from the line used for RNA-seq analysis.

761 **Additional files**

762 **Additional file 1: Table S1.** Antibodies used in immunocytochemistry and immunoblotting
763 experiments (XLSX).

764 **Additional file 2: Figures S1-S5.** Figure legends provided in file (PDF).

765 **Additional file 3: Table S2.** DEGs from pairwise comparisons of the four sample types for
766 cExN or cIN NPCs (XLSX).

767 **Additional file 4: Table S3.** Hierarchical clustering of the relative expression of DEGs across
768 the four sample types for cExN and cIN NPCs was performed using ClustVis. Order of genes in
769 the cluster and unit variance scaled relative expression values are indicated (XLSX).

770 **Additional file 5: Table S4.** Details about selected DEGs within IPA networks (PDF).

771 **Additional file 6: Table S5.** cExN DEG comparison to other studies (XLSX).

772

773

774

775

776

777

778

779

780

781

782 **References**

783 1. Wing L, Gould J. Severe impairments of social interaction and associated abnormalities
784 in children: epidemiology and classification. J Autism Dev Disord. 1979;9(1):11-29.
785 2. Gaugler T, Klei L, Sanders SJ, Bodea CA, Goldberg AP, Lee AB, et al. Most genetic risk
786 for autism resides with common variation. Nat Genet. 2014;46(8):881-5.
787 3. Donovan AP, Basson MA. The neuroanatomy of autism - a developmental perspective. J
788 Anat. 2017;230(1):4-15.
789 4. Ecker C, Bookheimer SY, Murphy DG. Neuroimaging in autism spectrum disorder: brain
790 structure and function across the lifespan. Lancet Neurol. 2015;14(11):1121-34.
791 5. Zikopoulos B, Barbas H. Altered neural connectivity in excitatory and inhibitory cortical
792 circuits in autism. Front Hum Neurosci. 2013;7:609.
793 6. Canitano R, Pallagrosi M. Autism Spectrum Disorders and Schizophrenia Spectrum
794 Disorders: Excitation/Inhibition Imbalance and Developmental Trajectories. Front Psychiatry.
795 2017;8:69.
796 7. DeRosa BA, El Hokayem J, Artimovich E, Garcia-Serje C, Phillips AW, Van Booven D,
797 et al. Convergent Pathways in Idiopathic Autism Revealed by Time Course Transcriptomic
798 Analysis of Patient-Derived Neurons. Sci Rep. 2018;8(1):8423.
799 8. Liu X, Campanac E, Cheung HH, Ziats MN, Canterel-Thouennon L, Raygada M, et al.
800 Idiopathic Autism: Cellular and Molecular Phenotypes in Pluripotent Stem Cell-Derived Neurons.
801 Mol Neurobiol. 2017;54(6):4507-23.
802 9. Aksoy I, Utami KH, Winata CL, Hillmer AM, Rouam SL, Briault S, et al. Personalized
803 genome sequencing coupled with iPSC technology identifies GTDC1 as a gene involved in
804 neurodevelopmental disorders. Hum Mol Genet. 2017;26(2):367-82.

805 10. Griesi-Oliveira K, Acab A, Gupta AR, Sunaga DY, Chailangkarn T, Nicol X, et al.
806 Modeling non-syndromic autism and the impact of TRPC6 disruption in human neurons. Mol
807 Psychiatry. 2015;20(11):1350-65.
808 11. Deshpande A, Yadav S, Dao DQ, Wu ZY, Hokanson KC, Cahill MK, et al. Cellular
809 Phenotypes in Human iPSC-Derived Neurons from a Genetic Model of Autism Spectrum
810 Disorder. Cell Rep. 2017;21(10):2678-87.
811 12. Kathuria A, Nowosiad P, Jagasia R, Aigner S, Taylor RD, Andreae LC, et al. Stem cell-
812 derived neurons from autistic individuals with SHANK3 mutation show morphogenetic
813 abnormalities during early development. Mol Psychiatry. 2018;23(3):735-46.
814 13. Wang P, Lin M, Pedrosa E, Hrabovsky A, Zhang Z, Guo W, et al. CRISPR/Cas9-
815 mediated heterozygous knockout of the autism gene CHD8 and characterization of its
816 transcriptional networks in neurodevelopment. Mol Autism. 2015;6:55.
817 14. Wang P, Mokhtari R, Pedrosa E, Kirschenbaum M, Bayrak C, Zheng D, et al.
818 CRISPR/Cas9-mediated heterozygous knockout of the autism gene CHD8 and characterization
819 of its transcriptional networks in cerebral organoids derived from iPS cells. Mol Autism.
820 2017;8:11.
821 15. Woodbury-Smith M, Deneault E, Yuen RKC, Walker S, Zarrei M, Pellecchia G, et al.
822 Mutations in RAB39B in individuals with intellectual disability, autism spectrum disorder, and
823 macrocephaly. Mol Autism. 2017;8:59.
824 16. Deneault E, White SH, Rodrigues DC, Ross PJ, Faheem M, Zaslavsky K, et al.
825 Complete Disruption of Autism-Susceptibility Genes by Gene Editing Predominantly Reduces
826 Functional Connectivity of Isogenic Human Neurons. Stem Cell Reports. 2018;11(5):1211-25.
827 17. Russo FB, Freitas BC, Pignatari GC, Fernandes IR, Sebat J, Muotri AR, et al. Modeling
828 the Interplay Between Neurons and Astrocytes in Autism Using Human Induced Pluripotent
829 Stem Cells. Biol Psychiatry. 2018;83(7):569-78.

830 18. Marchetto MC, Belinson H, Tian Y, Freitas BC, Fu C, Vadodaria K, et al. Altered
831 proliferation and networks in neural cells derived from idiopathic autistic individuals. Mol
832 Psychiatry. 2017;22(6):820-35.
833 19. Mariani J, Coppola G, Zhang P, Abyzov A, Provini L, Tomasini L, et al. FOXG1-
834 Dependent Dysregulation of GABA/Glutamate Neuron Differentiation in Autism Spectrum
835 Disorders. Cell. 2015;162(2):375-90.
836 20. Schafer ST, Paquola ACM, Stern S, Gosselin D, Ku M, Pena M, et al. Pathological
837 priming causes developmental gene network heterochronicity in autistic subject-derived
838 neurons. Nat Neurosci. 2019.
839 21. Christensen DL, Baio J, Van Naarden Braun K, Bilder D, Charles J, Constantino JN, et
840 al. Prevalence and Characteristics of Autism Spectrum Disorder Among Children Aged 8 Years-
841 -Autism and Developmental Disabilities Monitoring Network, 11 Sites, United States, 2012.
842 MMWR Surveill Summ. 2016;65(3):1-23.
843 22. Constantino JN, Todorov A, Hilton C, Law P, Zhang Y, Molloy E, et al. Autism
844 recurrence in half siblings: strong support for genetic mechanisms of transmission in ASD.
845 Molecular psychiatry. 2013;18(2):137-8.
846 23. Gronborg TK, Schendel DE, Parner ET. Recurrence of autism spectrum disorders in full-
847 and half-siblings and trends over time: a population-based cohort study. JAMA Pediatr.
848 2013;167(10):947-53.
849 24. Constantino JN. Recurrence rates in autism spectrum disorders. Jama.
850 2014;312(11):1154-5.
851 25. Constantino JN, Zhang Y, Frazier T, Abbacchi AM, Law P. Sibling recurrence and the
852 genetic epidemiology of autism. The American journal of psychiatry. 2010;167(11):1349-56.
853 26. Ozonoff S, Young GS, Carter A, Messinger D, Yirmiya N, Zwaigenbaum L, et al.
854 Recurrence risk for autism spectrum disorders: a Baby Siblings Research Consortium study.
855 Pediatrics. 2011;128(3):e488-95.

856 27. De Rubeis S, He X, Goldberg AP, Poultney CS, Samocha K, Cicek AE, et al. Synaptic,
857 transcriptional and chromatin genes disrupted in autism. Nature. 2014;515(7526):209-15.
858 28. Mefford HC, Batshaw ML, Hoffman EP. Genomics, intellectual disability, and autism. N
859 Engl J Med. 2012;366(8):733-43.
860 29. Turner TN, Eichler EE. The Role of De Novo Noncoding Regulatory Mutations in
861 Neurodevelopmental Disorders. Trends Neurosci. 2018.
862 30. Williams SM, An JY, Edson J, Watts M, Murigneux V, Whitehouse AJO, et al. An
863 integrative analysis of non-coding regulatory DNA variations associated with autism spectrum
864 disorder. Mol Psychiatry. 2018.
865 31. Griesi-Oliveira K, Sertie AL. Autism spectrum disorders: an updated guide for genetic
866 counseling. Einstein (Sao Paulo). 2017;15(2):233-8.
867 32. Retterer K, Juusola J, Cho MT, Vitazka P, Millan F, Gibellini F, et al. Clinical application
868 of whole-exome sequencing across clinical indications. Genet Med. 2016;18(7):696-704.
869 33. Meganathan K, Lewis EMA, Gontarz P, Liu S, Stanley EG, Elefanty AG, et al.
870 Regulatory networks specifying cortical interneurons from human embryonic stem cells reveal
871 roles for CHD2 in interneuron development. Proc Natl Acad Sci U S A. 2017;114(52):E11180-
872 E9.
873 34. Lunden JW, Durens M, Phillips AW, Nestor MW. Cortical interneuron function in autism
874 spectrum condition. Pediatr Res. 2019;85(2):146-54.
875 35. Hoekstra SD, Stringer S, Heine VM, Posthuma D. Genetically-Informed Patient Selection
876 for iPSC Studies of Complex Diseases May Aid in Reducing Cellular Heterogeneity. Front Cell
877 Neurosci. 2017;11:164.
878 36. SFARI gene Database. https://www.sfari.org/resource/sfari-gene/. Accessed December
879 2018.

880 37. Weiner DJ, Wigdor EM, Ripke S, Walters RK, Kosmicki JA, Grove J, et al. Polygenic
881 transmission disequilibrium confirms that common and rare variation act additively to create risk
882 for autism spectrum disorders. Nat Genet. 2017;49(7):978-85.
883 38. Wang DB, Kinoshita C, Kinoshita Y, Morrison RS. p53 and mitochondrial function in
884 neurons. Biochim Biophys Acta. 2014;1842(8):1186-97.
885 39. Liu Y, Clegg HV, Leslie PL, Di J, Tollini LA, He Y, et al. CHCHD2 inhibits apoptosis by
886 interacting with Bcl-x L to regulate Bax activation. Cell Death Differ. 2015;22(6):1035-46.
887 40. Solito E, McArthur S, Christian H, Gavins F, Buckingham JC, Gillies GE. Annexin A1 in
888 the brain--undiscovered roles? Trends Pharmacol Sci. 2008;29(3):135-42.
889 41. Correia CT, Conceicao IC, Oliveira B, Coelho J, Sousa I, Sequeira AF, et al. Recurrent
890 duplications of the annexin A1 gene (ANXA1) in autism spectrum disorders. Mol Autism.
891 2014;5(1):28.
892 42. Parente L, Solito E. Annexin 1: more than an anti-phospholipase protein. Inflamm Res.
893 2004;53(4):125-32.
894 43. Toyoshima M, Akamatsu W, Okada Y, Ohnishi T, Balan S, Hisano Y, et al. Analysis of
895 induced pluripotent stem cells carrying 22q11.2 deletion. Transl Psychiatry. 2016;6(11):e934.
896 44. Chailangkarn T, Trujillo CA, Freitas BC, Hrvoj-Mihic B, Herai RH, Yu DX, et al. A human
897 neurodevelopmental model for Williams syndrome. Nature. 2016;536(7616):338-43.
898 45. Friocourt G, Poirier K, Rakic S, Parnavelas JG, Chelly J. The role of ARX in cortical
899 development. Eur J Neurosci. 2006;23(4):869-76.
900 46. Zhang Y, Hoxha E, Zhao T, Zhou X, Alvarez-Bolado G. Foxb1 Regulates Negatively the
901 Proliferation of Oligodendrocyte Progenitors. Front Neuroanat. 2017;11:53.
902 47. Takebayashi-Suzuki K, Kitayama A, Terasaka-Iioka C, Ueno N, Suzuki A. The forkhead
903 transcription factor FoxB1 regulates the dorsal-ventral and anterior-posterior patterning of the
904 ectoderm during early Xenopus embryogenesis. Dev Biol. 2011;360(1):11-29.

905 48. Kobeissy FH, Hansen K, Neumann M, Fu S, Jin K, Liu J. Deciphering the Role of Emx1
906 in Neurogenesis: A Neuroproteomics Approach. Front Mol Neurosci. 2016;9:98.
907 49. Hattori S, Takao K, Tanda K, Toyama K, Shintani N, Baba A, et al. Comprehensive
908 behavioral analysis of pituitary adenylate cyclase-activating polypeptide (PACAP) knockout
909 mice. Front Behav Neurosci. 2012;6:58.
910 50. Shintani N, Hashimoto H, Tanaka K, Kawagishi N, Kawaguchi C, Hatanaka M, et al.
911 Serotonergic inhibition of intense jumping behavior in mice lacking PACAP (Adcyap1-/-). Ann N
912 Y Acad Sci. 2006;1070:545-9.
913 51. Gogos JA, Morgan M, Luine V, Santha M, Ogawa S, Pfaff D, et al. Catechol-O-
914 methyltransferase-deficient mice exhibit sexually dimorphic changes in catecholamine levels
915 and behavior. Proc Natl Acad Sci U S A. 1998;95(17):9991-6.
916 52. Qayyum A, Zai CC, Hirata Y, Tiwari AK, Cheema S, Nowrouzi B, et al. The Role of the
917 Catechol-o-Methyltransferase (COMT) GeneVal158Met in Aggressive Behavior, a Review of
918 Genetic Studies. Curr Neuropharmacol. 2015;13(6):802-14.
919 53. Bowers ME, Ressler KJ. Sex-dependence of anxiety-like behavior in cannabinoid
920 receptor 1 (Cnr1) knockout mice. Behav Brain Res. 2016;300:65-9.
921 54. Paes LA, Torre OHD, Henriques TB, de Mello MP, Celeri E, Dalgalarrondo P, et al.
922 Association between serotonin 2C receptor gene (HTR2C) polymorphisms and
923 psychopathological symptoms in children and adolescents. Braz J Med Biol Res.
924 2018;51(8):e7252.
925 55. Martin CB, Ramond F, Farrington DT, Aguiar AS, Jr., Chevarin C, Berthiau AS, et al.
926 RNA splicing and editing modulation of 5-HT(2C) receptor function: relevance to anxiety and
927 aggression in VGV mice. Mol Psychiatry. 2013;18(6):656-65.
928 56. Shaltiel G, Maeng S, Malkesman O, Pearson B, Schloesser RJ, Tragon T, et al.
929 Evidence for the involvement of the kainate receptor subunit GluR6 (GRIK2) in mediating

930 behavioral displays related to behavioral symptoms of mania. Mol Psychiatry. 2008;13(9):858-
931 72.
932 57. Stratinaki M, Varidaki A, Mitsi V, Ghose S, Magida J, Dias C, et al. Regulator of G
933 protein signaling 4 [corrected] is a crucial modulator of antidepressant drug action in depression
934 and neuropathic pain models. Proc Natl Acad Sci U S A. 2013;110(20):8254-9.
935 58. Chen J, Yu S, Fu Y, Li X. Synaptic proteins and receptors defects in autism spectrum
936 disorders. Front Cell Neurosci. 2014;8:276.
937 59. Tsai NP, Huber KM. Protocadherins and the Social Brain. Biol Psychiatry.
938 2017;81(3):173-4.
939 60. Washbourne P, Dityatev A, Scheiffele P, Biederer T, Weiner JA, Christopherson KS, et
940 al. Cell adhesion molecules in synapse formation. J Neurosci. 2004;24(42):9244-9.
941 61. Wang X, Weiner JA, Levi S, Craig AM, Bradley A, Sanes JR. Gamma protocadherins
942 are required for survival of spinal interneurons. Neuron. 2002;36(5):843-54.
943 62. Bruining H, Matsui A, Oguro-Ando A, Kahn RS, Van't Spijker HM, Akkermans G, et al.
944 Genetic Mapping in Mice Reveals the Involvement of Pcdh9 in Long-Term Social and Object
945 Recognition and Sensorimotor Development. Biol Psychiatry. 2015;78(7):485-95.
946 63. Martin EA, Muralidhar S, Wang Z, Cervantes DC, Basu R, Taylor MR, et al. Correction:
947 The intellectual disability gene Kirrel3 regulates target-specific mossy fiber synapse
948 development in the hippocampus. Elife. 2016;5.
949 64. Mohebiany AN, Harroch S, Bouyain S. New insights into the roles of the contactin cell
950 adhesion molecules in neural development. Adv Neurobiol. 2014;8:165-94.
951 65. Karayannis T, Au E, Patel JC, Kruglikov I, Markx S, Delorme R, et al. Cntnap4
952 differentially contributes to GABAergic and dopaminergic synaptic transmission. Nature.
953 2014;511(7508):236-40.
954 66. Adams JC, Lawler J. The thrombospondins. Cold Spring Harb Perspect Biol.
955 2011;3(10):a009712.

956 67. Rubinstein M, Patowary A, Stanaway IB, McCord E, Nesbitt RR, Archer M, et al.
957 Association of rare missense variants in the second intracellular loop of NaV1.7 sodium
958 channels with familial autism. Mol Psychiatry. 2018;23(2):231-9.
959 68. Soto D, Altafaj X, Sindreu C, Bayes A. Glutamate receptor mutations in psychiatric and
960 neurodevelopmental disorders. Commun Integr Biol. 2014;7(1):e27887.
961 69. Contractor A, Mulle C, Swanson GT. Kainate receptors coming of age: milestones of two
962 decades of research. Trends Neurosci. 2011;34(3):154-63.
963 70. Kim SA, Kim JH, Park M, Cho IH, Yoo HJ. Family-based association study between
964 GRIK2 polymorphisms and autism spectrum disorders in the Korean trios. Neurosci Res.
965 2007;58(3):332-5.
966 71. Pravetoni M, Wickman K. Behavioral characterization of mice lacking GIRK/Kir3 channel
967 subunits. Genes Brain Behav. 2008;7(5):523-31.
968 72. Guglielmi L, Servettini I, Caramia M, Catacuzzeno L, Franciolini F, D'Adamo MC, et al.
969 Update on the implication of potassium channels in autism: K(+) channelautism spectrum
970 disorder. Front Cell Neurosci. 2015;9:34.
971 73. Binda A, Rivolta I, Villa C, Chisci E, Beghi M, Cornaggia CM, et al. A Novel KCNJ2
972 Mutation Identified in an Autistic Proband Affects the Single Channel Properties of Kir2.1. Front
973 Cell Neurosci. 2018;12:76.
974 74. Ramanathan S, Woodroffe A, Flodman PL, Mays LZ, Hanouni M, Modahl CB, et al. A
975 case of autism with an interstitial deletion on 4q leading to hemizygosity for genes encoding for
976 glutamine and glycine neurotransmitter receptor sub-units (AMPA 2, GLRA3, GLRB) and
977 neuropeptide receptors NPY1R, NPY5R. BMC Med Genet. 2004;5:10.
978 75. Gu X, Zhou L, Lu W. An NMDA Receptor-Dependent Mechanism Underlies Inhibitory
979 Synapse Development. Cell Rep. 2016;14(3):471-8.
980 76. Perez-Garcia CG. ErbB4 in Laminated Brain Structures: A Neurodevelopmental
981 Approach to Schizophrenia. Front Cell Neurosci. 2015;9:472.

982 77. Yau HJ, Wang HF, Lai C, Liu FC. Neural development of the neuregulin receptor ErbB4
983 in the cerebral cortex and the hippocampus: preferential expression by interneurons tangentially
984 migrating from the ganglionic eminences. Cereb Cortex. 2003;13(3):252-64.
985 78. Yaguchi K, Nishimura-Akiyoshi S, Kuroki S, Onodera T, Itohara S. Identification of
986 transcriptional regulatory elements for Ntng1 and Ntng2 genes in mice. Mol Brain. 2014;7:19.
987 79. Caubit X, Gubellini P, Andrieux J, Roubertoux PL, Metwaly M, Jacq B, et al. TSHZ3
988 deletion causes an autism syndrome and defects in cortical projection neurons. Nat Genet.
989 2016;48(11):1359-69.
990 80. Sleven H, Welsh SJ, Yu J, Churchill MEA, Wright CF, Henderson A, et al. De Novo
991 Mutations in EBF3 Cause a Neurodevelopmental Syndrome. Am J Hum Genet.
992 2017;100(1):138-50.
993 81. Blanchet P, Bebin M, Bruet S, Cooper GM, Thompson ML, Duban-Bedu B, et al. MYT1L
994 mutations cause intellectual disability and variable obesity by dysregulating gene expression
995 and development of the neuroendocrine hypothalamus. PLoS Genet. 2017;13(8):e1006957.
996 82. Stevens SJ, van Ravenswaaij-Arts CM, Janssen JW, Klein Wassink-Ruiter JS, van
997 Essen AJ, Dijkhuizen T, et al. MYT1L is a candidate gene for intellectual disability in patients
998 with 2p25.3 (2pter) deletions. Am J Med Genet A. 2011;155A(11):2739-45.
999 83. Germain ND, Chen PF, Plocik AM, Glatt-Deeley H, Brown J, Fink JJ, et al. Gene
1000 expression analysis of human induced pluripotent stem cell-derived neurons carrying copy
1001 number variants of chromosome 15q11-q13.1. Mol Autism. 2014;5:44.
1002 84. Wang P, Zhao D, Lachman HM, Zheng D. Enriched expression of genes associated with
1003 autism spectrum disorders in human inhibitory neurons. Transl Psychiatry. 2018;8(1):13.
1004 85. Nguyen NH, Brathe A, Hassel B. Neuronal uptake and metabolism of glycerol and the
1005 neuronal expression of mitochondrial glycerol-3-phosphate dehydrogenase. J Neurochem.
1006 2003;85(4):831-42.

1007 86. Barge-Schaapveld DQ, Ofman R, Knegt AC, Alders M, Hohne W, Kemp S, et al.
1008 Intellectual disability and hemizygous GPD2 mutation. Am J Med Genet A. 2013;161A(5):1044-
1009 50.
1010 87. Daoud H, Gruchy N, Constans JM, Moussaoui E, Saumureau S, Bayou N, et al.
1011 Haploinsufficiency of the GPD2 gene in a patient with nonsyndromic mental retardation. Hum
1012 Genet. 2009;124(6):649-58.
1013 88. Sahakyan A, Kim R, Chronis C, Sabri S, Bonora G, Theunissen TW, et al. Human Naive
1014 Pluripotent Stem Cells Model X Chromosome Dampening and X Inactivation. Cell Stem Cell.
1015 2017;20(1):87-101.
1016 89. Dandulakis MG, Meganathan K, Kroll KL, Bonni A, Constantino JN. Complexities of X
1017 chromosome inactivation status in female human induced pluripotent stem cells-a brief review
1018 and scientific update for autism research. J Neurodev Disord. 2016;8:22.
1019 90. Tukiainen T, Villani AC, Yen A, Rivas MA, Marshall JL, Satija R, et al. Landscape of X
1020 chromosome inactivation across human tissues. Nature. 2017;550(7675):244-8.
1021 91. Gershoni M, Pietrokovski S. The landscape of sex-differential transcriptome and its
1022 consequent selection in human adults. BMC Biol. 2017;15(1):7.
1023

Table 1

Clinical characteristic	AP	IS	UM
Age of ASD diagnostic confirmation	3.5 years	18 years	N/A
Social Responsiveness Scale-2	83T	72T	56T (spouse-report)
Depression and Anxiety	Yes	Yes	No
Seizure history	No	No	No
Developmental delay	Yes	No	No
Eye contact	Poor	Fair	Good
Repetitive behavior	Yes	No	No
Abnormal sensory sensitivities	Yes	No	No
IQ	65	102 (Raven)	108 (Raven)
Speech delay	Yes	No	No
ASD	Severe	Moderate	No
Intellectual Disability	Yes	No	No
Mutation location	GPD2 chr2:157352686 (hg19) G>A p.G78E, c.233G>A	GPD2 chr2:157352686 (hg19) G>A p.G78E, c.233G>A	GPD2 chr2:157352686 (hg19) G>A p.G78E, c.233G>A

Fig. 1

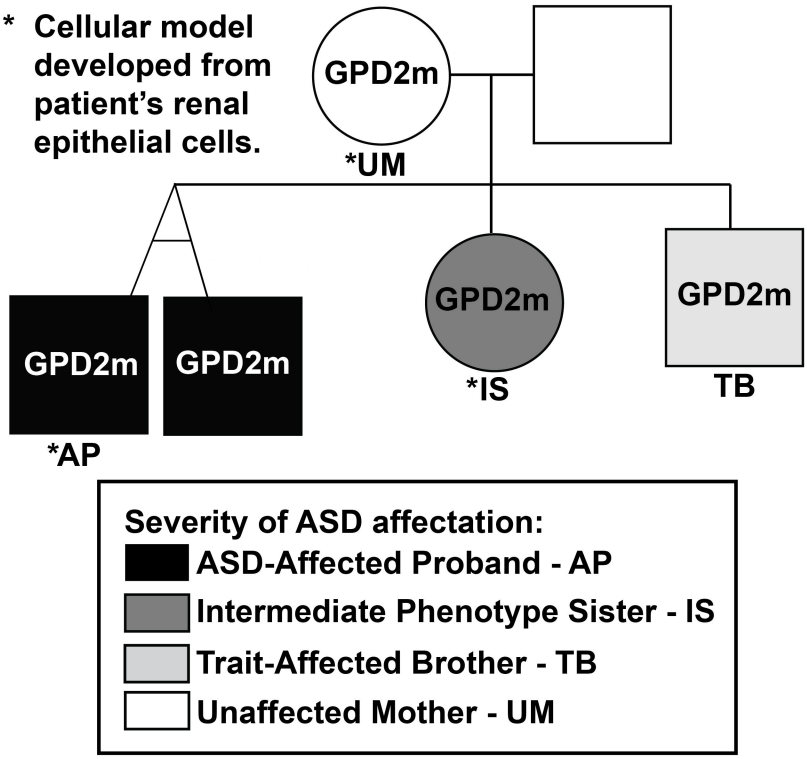
* Cellular model developed from patient's renal epithelial cells.
GPD2m
*UM
GPD2m
GPD2m
*AP
GPD2m
*IS
GPD2m
TB
Severity of ASD affectation:
ASD-Affected Proband - AP
Intermediate Phenotype Sister - IS
Trait-Affected Brother - TB
Unaffected Mother - UM

Fig. 2

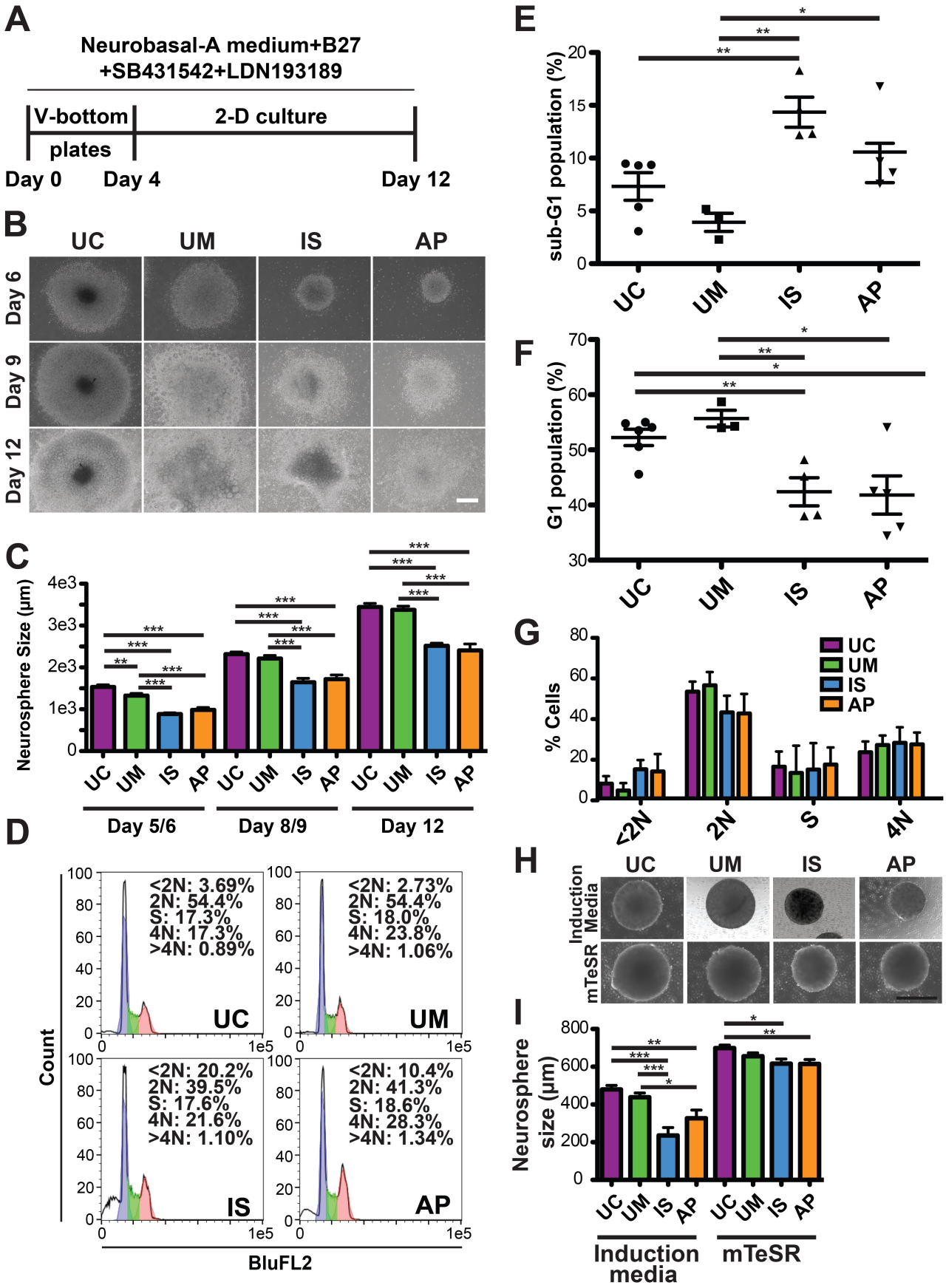
A
Neurobasal-A medium+B27
+SB431542+LDN193189
V-bottom plates
2-D culture
Day 0
Day 4
Day 12
B
UC
UM
IS
AP
Day 6
Day 9
Day 12
C
Neurosphere Size (μm)
Day 5/6
Day 8/9
Day 12
D
Count
BluFL2
<2N: 3.69%
2N: 54.4%
S: 17.3%
4N: 17.3%
>4N: 0.89%
UC
<2N: 2.73%
2N: 54.4%
S: 18.0%
4N: 23.8%
>4N: 1.06%
UM
<2N: 20.2%
2N: 39.5%
S: 17.6%
4N: 21.6%
>4N: 1.10%
IS
<2N: 10.4%
2N: 41.3%
S: 18.6%
4N: 28.3%
>4N: 1.34%
AP
E
sub-G1 population (%)
F
G1 population (%)
G
% Cells
<2N
2N
S
4N
H
Induction Media
mTeSR
I
Neurosphere size (μm)
Induction media
mTeSR

Fig. 3

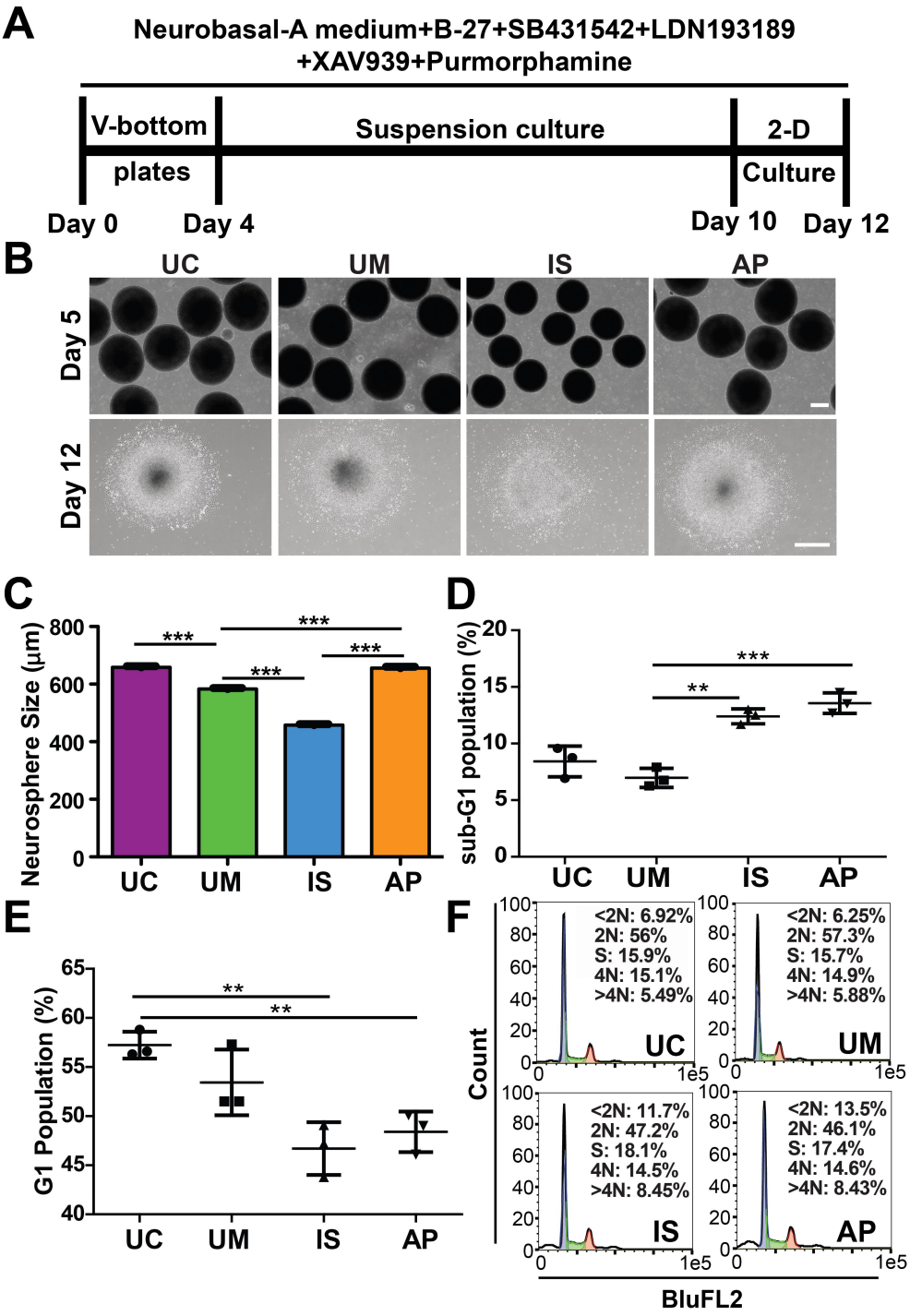
A
Neurobasal-A medium+B-27+SB431542+LDN193189
+XAV939+Purmorphamine
V-bottom
plates
Suspension culture
2-D
Culture
Day 0
Day 4
Day 10
Day 12
B
UC
UM
IS
AP
Day 5
Day 12
C
Neurosphere Size (μm)
800
600
400
200
0
***
***
***
***
UC
UM
IS
AP
D
sub-G1 population (%)
20
15
10
5
0
***
**
UC
UM
IS
AP
E
G1 Population (%)
65
60
55
50
45
40
**
**
UC
UM
IS
AP
F
Count
<2N: 6.92%
2N: 56%
S: 15.9%
4N: 15.1%
>4N: 5.49%
UC
<2N: 6.25%
2N: 57.3%
S: 15.7%
4N: 14.9%
>4N: 5.88%
UM
<2N: 11.7%
2N: 47.2%
S: 18.1%
4N: 14.5%
>4N: 8.45%
IS
<2N: 13.5%
2N: 46.1%
S: 17.4%
4N: 14.6%
>4N: 8.43%
AP
100
80
60
40
20
0
1e5
BluFL2

Fig. 4

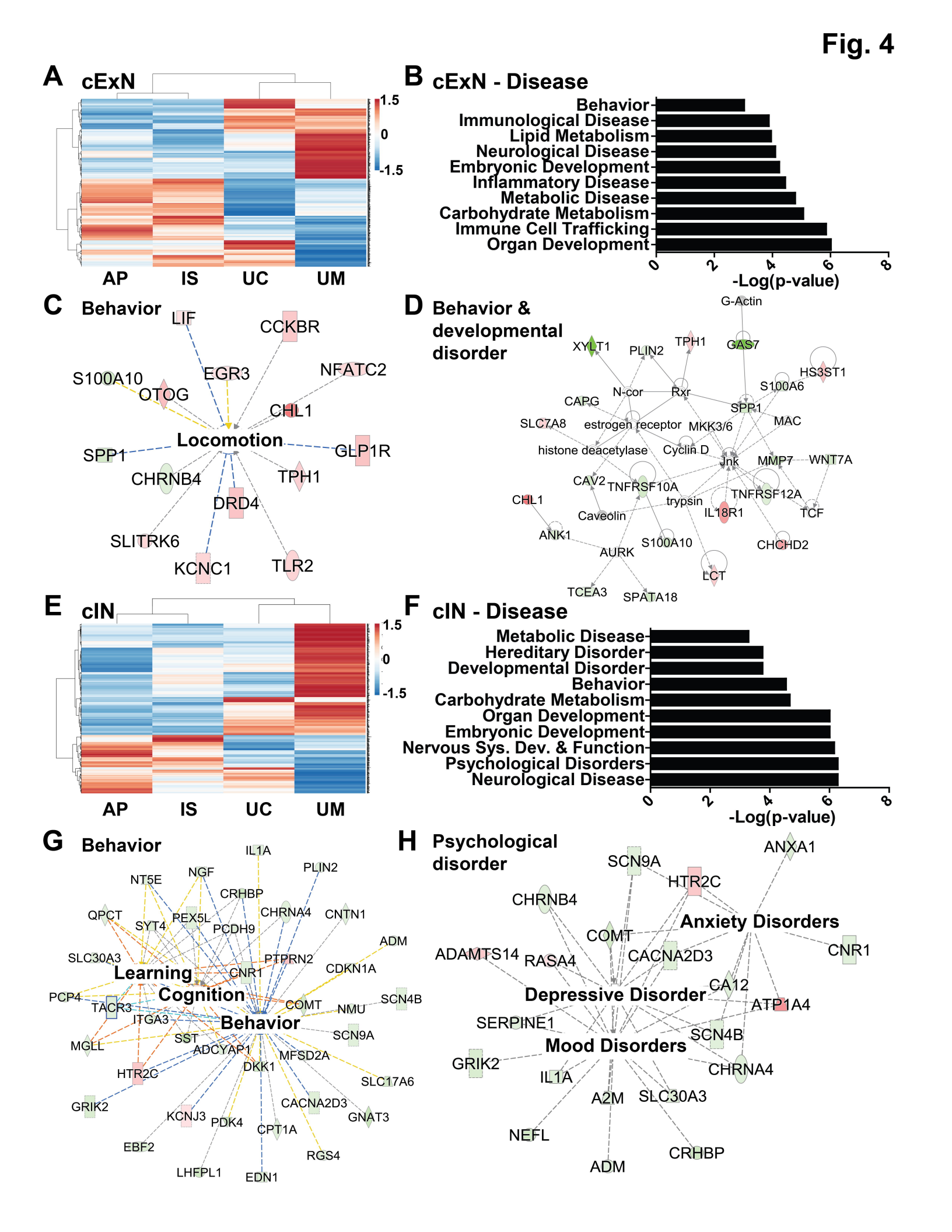
A
cExN
1.5
0
-1.5
AP
IS
UC
UM
B
cExN - Disease
Behavior
Immunological Disease
Lipid Metabolism
Neurological Disease
Embryonic Development
Inflammatory Disease
Metabolic Disease
Carbohydrate Metabolism
Immune Cell Trafficking
Organ Development
0
2
4
6
8
-Log(p-value)
C
Behavior
LIF
CCKBR
S100A10
EGR3
NFATC2
OTOG
CHL1
Locomotion
SPP1
GLP1R
CHRNB4
TPH1
DRD4
SLITRK6
KCNC1
TLR2
D
Behavior &
developmental
disorder
G-Actin
XYLT1
PLIN2
TPH1
GAS7
HS3ST1
S100A6
N-cor
Rxr
CAPG
SPP1
SLC7A8
estrogen receptor
MKK3/6
MAC
histone deacetylase
Cyclin D
Jnk
MMP7
WNT7A
CAV2
TNFRSF10A
TNFRSF12A
CHL1
trypsin
Caveolin
IL18R1
TCF
ANK1
S100A10
CHCHD2
AURK
LCT
TCEA3
SPATA18
E
cIN
1.5
0
-1.5
AP
IS
UC
UM
F
cIN - Disease
Metabolic Disease
Hereditary Disorder
Developmental Disorder
Behavior
Carbohydrate Metabolism
Organ Development
Embryonic Development
Nervous Sys. Dev. & Function
Psychological Disorders
Neurological Disease
0
2
4
6
8
-Log(p-value)
G
Behavior
IL1A
NT5E
NGF
PLIN2
CRHBP
QPCT
PEX5L
CHRNA4
CNTN1
SYT4
PCDH9
ADM
SLC30A3
PTPRN2
Learning
CNR1
CDKN1A
PCP4
Cognition
SCN4B
TACR3
COMT
NMU
ITGA3
Behavior
SST
SCN9A
MGLL
ADCYAP1
MFSD2A
DKK1
HTR2C
SLC17A6
GRIK2
CACNA2D3
KCNJ3
GNAT3
PDK4
CPT1A
EBF2
RGS4
LHFPL1
EDN1
H
Psychological
disorder
ANXA1
SCN9A
HTR2C
CHRNB4
Anxiety Disorders
COMT
CNR1
ADAMTS14
RASA4
CACNA2D3
CA12
Depressive Disorder
ATP1A4
SERPINE1
SCN4B
Mood Disorders
GRIK2
CHRNA4
IL1A
A2M
SLC30A3
NEFL
CRHBP
ADM

Fig. 5

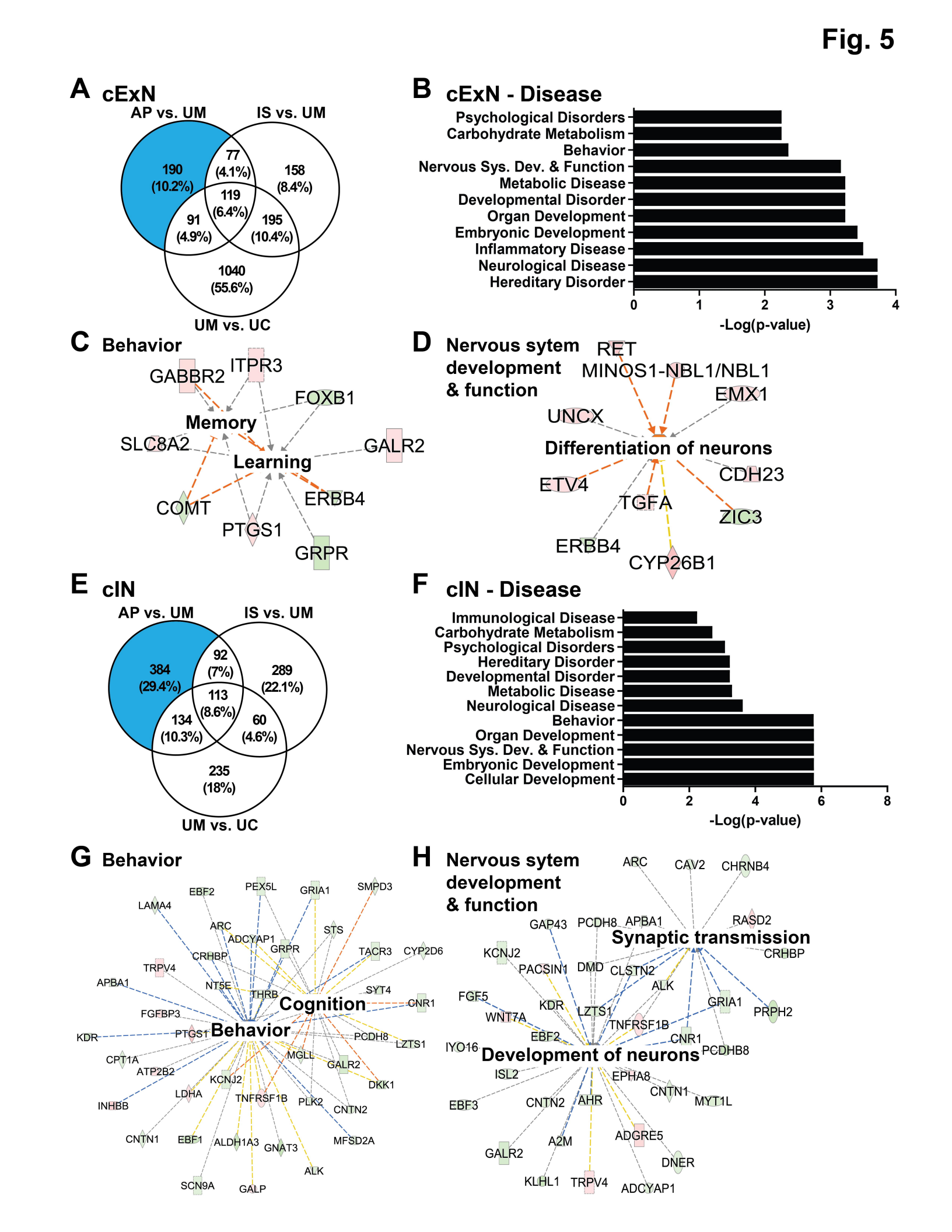
A cExN
AP vs. UM
IS vs. UM
UM vs. UC
190 (10.2%)
77 (4.1%)
158 (8.4%)
119 (6.4%)
91 (4.9%)
195 (10.4%)
1040 (55.6%)
B cExN - Disease
Psychological Disorders
Carbohydrate Metabolism
Behavior
Nervous Sys. Dev. & Function
Metabolic Disease
Developmental Disorder
Organ Development
Embryonic Development
Inflammatory Disease
Neurological Disease
Hereditary Disorder
0 1 2 3 4
-Log(p-value)
C Behavior
GABBR2
ITPR3
FOXB1
Memory
SLC8A2
GALR2
Learning
COMT
ERBB4
PTGS1
GRPR
D Nervous sytem development & function
RET
MINOS1-NBL1/NBL1
EMX1
UNCX
Differentiation of neurons
CDH23
ETV4
TGFA
ZIC3
ERBB4
CYP26B1
E cIN
AP vs. UM
IS vs. UM
UM vs. UC
384 (29.4%)
92 (7%)
289 (22.1%)
113 (8.6%)
134 (10.3%)
60 (4.6%)
235 (18%)
F cIN - Disease
Immunological Disease
Carbohydrate Metabolism
Psychological Disorders
Hereditary Disorder
Developmental Disorder
Metabolic Disease
Neurological Disease
Behavior
Organ Development
Nervous Sys. Dev. & Function
Embryonic Development
Cellular Development
0 2 4 6 8
-Log(p-value)
G Behavior
EBF2
PEX5L
GRIA1
SMPD3
LAMA4
ARC
ADCYAP1
STS
GRPR
CRHBP
TACR3
CYP2D6
TRPV4
APBA1
NT5E
THRB
SYT4
Cognition
CNR1
FGFBP3
KDR
PTGS1
Behavior
PCDH8
LZTS1
CPT1A
MGLL
ATP2B2
GALR2
KCNJ2
DKK1
LDHA
INHBB
TNFRSF1B
PLK2
CNTN2
CNTN1
EBF1
ALDH1A3
GNAT3
MFSD2A
ALK
SCN9A
GALP
H Nervous sytem development & function
ARC
CAV2
CHRNB4
GAP43
PCDH8
APBA1
RASD2
Synaptic transmission
KCNJ2
CRHBP
PACSIN1
DMD
CLSTN2
ALK
FGF5
KDR
LZTS1
GRIA1
PRPH2
WNT7A
TNFRSF1B
EBF2
CNR1
IYO16
Development of neurons
PCDHB8
ISL2
EPHA8
CNTN1
EBF3
CNTN2
AHR
MYT1L
ADGRE5
A2M
GALR2
DNER
KLHL1
TRPV4
ADCYAP1

Fig. 6

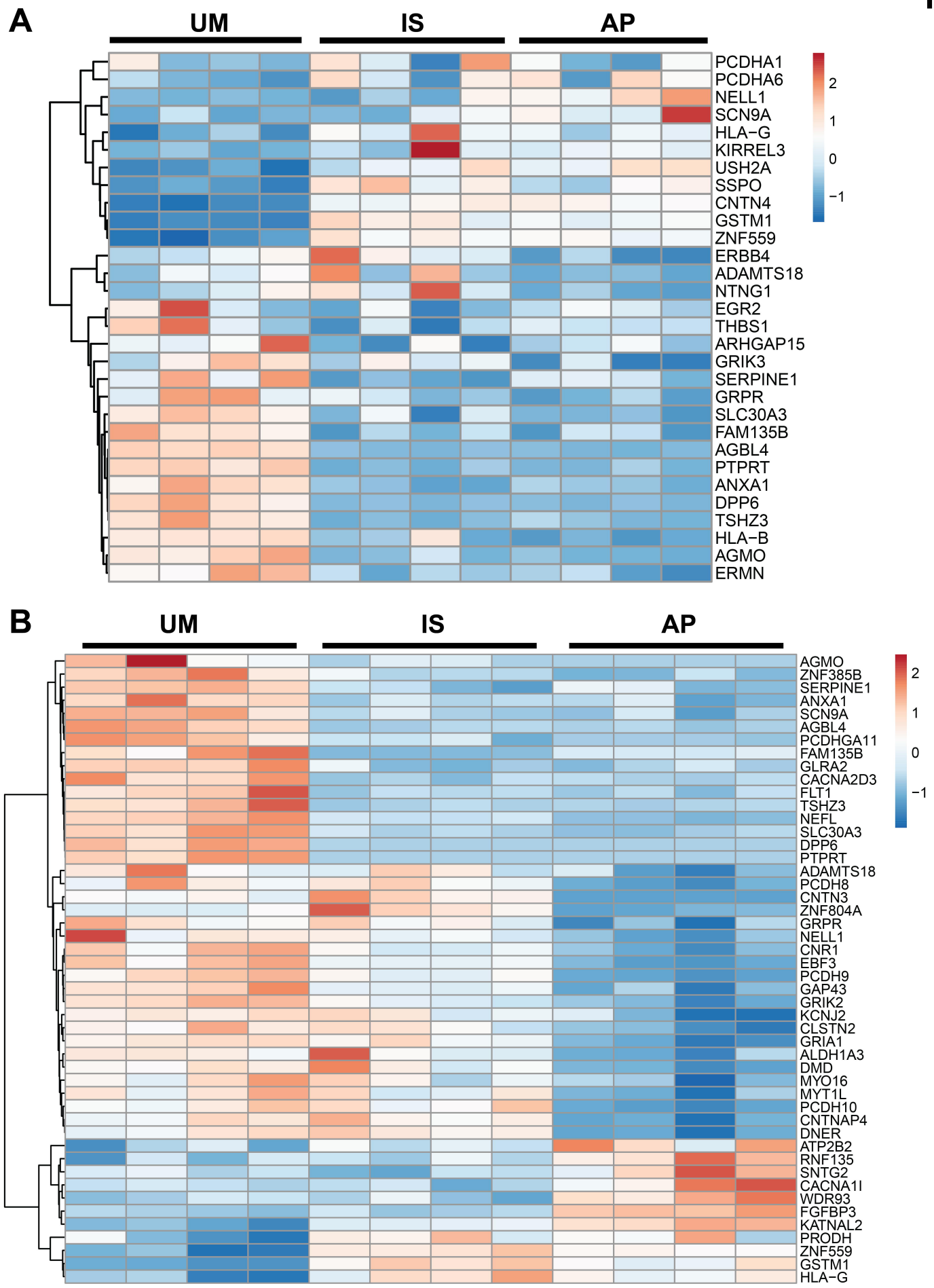
A
UM
IS
AP
PCDHA1
PCDHA6
NELL1
SCN9A
HLA−G
KIRREL3
USH2A
SSPO
CNTN4
GSTM1
ZNF559
ERBB4
ADAMTS18
NTNG1
EGR2
THBS1
ARHGAP15
GRIK3
SERPINE1
GRPR
SLC30A3
FAM135B
AGBL4
PTPRT
ANXA1
DPP6
TSHZ3
HLA−B
AGMO
ERMN
2
1
0
−1
B
UM
IS
AP
AGMO
ZNF385B
SERPINE1
ANXA1
SCN9A
AGBL4
PCDHGA11
FAM135B
GLRA2
CACNA2D3
FLT1
TSHZ3
NEFL
SLC30A3
DPP6
PTPRT
ADAMTS18
PCDH8
CNTN3
ZNF804A
GRPR
NELL1
CNR1
EBF3
PCDH9
GAP43
GRIK2
KCNJ2
CLSTN2
GRIA1
ALDH1A3
DMD
MYO16
MYT1L
PCDH10
CNTNAP4
DNER
ATP2B2
RNF135
SNTG2
CACNA1I
WDR93
FGFBP3
KATNAL2
PRODH
ZNF559
GSTM1
HLA−G
2
1
0
−1

Fig. 7

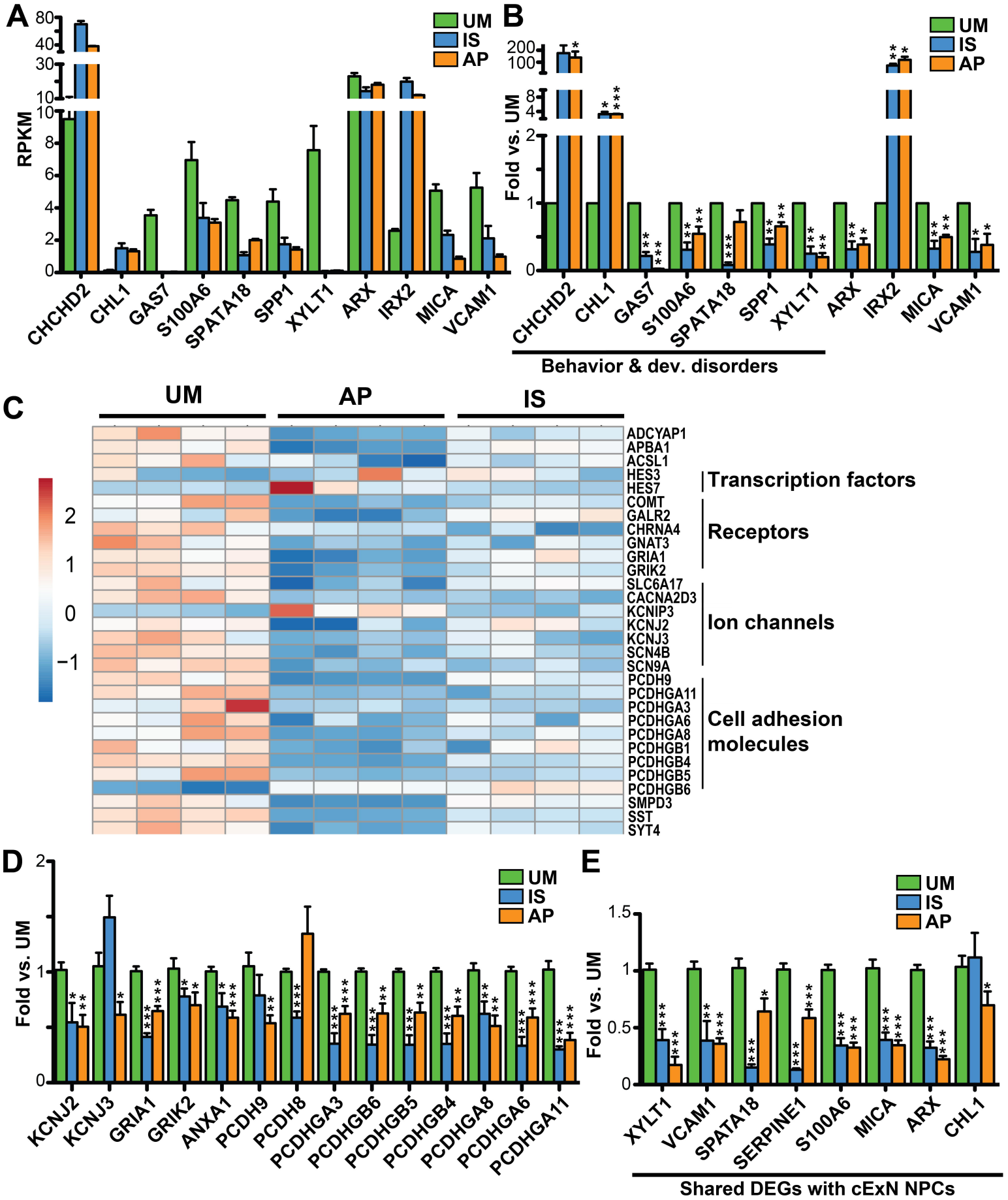
A
RPKM
UM
IS
AP
CHCHD2
CHL1
GAS7
S100A6
SPATA18
SPP1
XYLT1
ARX
IRX2
MICA
VCAM1
B
Fold vs. UM
Behavior & dev. disorders
C
UM
AP
IS
ADCYAP1
APBA1
ACSL1
HES3
HES7
COMT
GALR2
CHRNA4
GNAT3
GRIA1
GRIK2
SLC6A17
CACNA2D3
KCNIP3
KCNJ2
KCNJ3
SCN4B
SCN9A
PCDH9
PCDHGA11
PCDHGA3
PCDHGA6
PCDHGA8
PCDHGB1
PCDHGB4
PCDHGB5
PCDHGB6
SMPD3
SST
SYT4
Transcription factors
Receptors
Ion channels
Cell adhesion molecules
D
Fold vs. UM
KCNJ2
KCNJ3
GRIA1
GRIK2
ANXA1
PCDH9
PCDH8
PCDHGA3
PCDHGB6
PCDHGB5
PCDHGB4
PCDHGA8
PCDHGA6
PCDHGA11
E
Fold vs. UM
XYLT1
VCAM1
SPATA18
SERPINE1
S100A6
MICA
ARX
CHL1
Shared DEGs with cExN NPCs